Electronic Supplementary Material (ESI) for Journal of Materials Chemistry C.
This journal is © The Royal Society of Chemistry 2021

Alkyl chain regulation: distinctive odd-even effects of mechanoluminescence and room-temperature phosphorescence in alkyl substituted carbazole amide derivatives

Liangjing Tu[a], Weilong Che[a], Shuhui Li[a], Xiaoning Li[a], Yujun Xie,[a,b]* Zhen Li[a,c,d]*

[a]Institute of Molecular Aggregation Science, Tianjin University Tianjin 300072 (China). E-mail: xieyujun@tju.edu.cn; lizhentju@tju.edu.cn or lizhen@whu.edu.cn.
[b]Guangdong Provincial Key Laboratory of Luminescence from Molecular Aggregates (South China University of Techno-logy), Guangzhou 510640 (China).
[c]Tianjin Key Laboratory of Molecular Optoelectronic Sciences, Department of Chemistry, School of Science, Tianjin University, Tianjin 300072 (China).
[d]Department of Chemistry, Wuhan University Wuhan, Hubei 430072 (China).
[e]Joint School of National University of Singapore and Tianjin University, International Campus of Tianjin University Binhai New City, Fuzhou, Fujian 350207 (China).

Table of Content

General Remarks

Reagents and materials

Unless otherwise noted, all reagents used in the experiments are purchased from commercial sources without further purification. Carbazole is purchased from Damas-beta. For flash column chromatography, silica gel with 200 ~ 300 mesh is used. Sodium hydride is purchased from Innochem, which accounts for 60% dispersed in mineral oil.

Measurements

Analytical thin-layer chromatography (TLC) was performed using precoated TLC plates with silica gel GF-254. Nuclear magnetic resonance (^{1}H and ^{13}C NMR) spectra were obtained on a Bruker Ultra Shield plus 400 MHz spectrometer. Resonance patterns are reported with the notation s (singlet), d (double), t (triplet), q (quartet), and m (multiplet). Melting points were recorded on WRS-2C melting point meter. Thermogravimetric analyses (TGA) were recorded with a NETZSCH TG 209F3 thermal analyzer under nitrogen atmosphere with a heating rate of 20 ^{o}C min^{-1}. High-performance liquid chromatogram spectrum was recorded on Agilent 1100 HPLC. UV-vis spectra were performed on a Shimadzu UV-2600. The powder X-ray diffraction patterns were recorded by RIGAKU SMARTLAB9KW with an X-ray source of Cu Kα (λ = 1.5418 Å) at 298 K at 50 KV and 15 mA at a scan rate of 7° (2θ) min^{-1} (scan range: 5-50°). X-ray Single crystal diffraction for compounds data was performed on a diffractometer with CCD detector using Cu Kα radiation (λ= 1.5418 Å) source. Steady-state photoluminescence (PL) was measured by Hitachi F-4700. The lifetime and time-resolved emission spectra and PL quantum yield (PLQY) were obtained on Edinburgh FLS1000 fluorescence spectrophotometer. Luminescent photos and videos were taken by Huawei phone.

Synthesis and Characterization

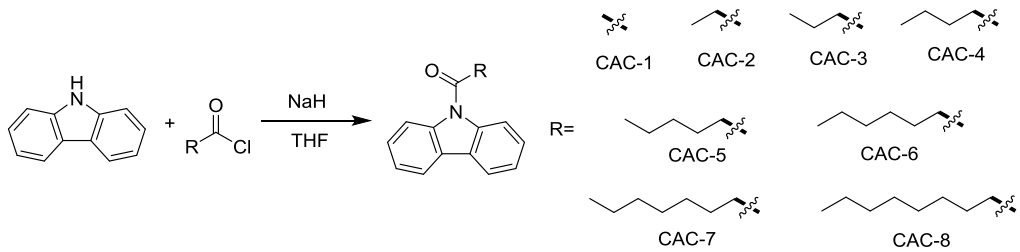

Scheme S1. Synthetic routes for CAC-*N* (*N* = 1 ~ 8)

1-(9H-carbazol-9-yl)ethan-1-one (CAC-1)

Carbazole (1.67 g, 10 mmol) and NaH (0.29 g, 12 mmol) were added into dry tetrahydrofuran (THF) solution (20 mL) at room temperature. After stirring for 30 min, the mixture was added dropwise to THF solution (20 mL) of acetyl chloride (1.07 mL, 15 mmol) at 0 °C. The mixture was further stirred for 5 h at room temperature before the reaction was quenched by pouring into water. The organic layer was extracted with CH_2Cl_2 for three times and dried with Na_2SO_4. After the solvent was removed by rotary evaporation, the residue was purified by column chromatography to give product as white solid (1.54 g, 78.2%).^{1}H NMR (400 MHz, Chloroform-*d*) δ 8.14 (d, *J* = 8.4 Hz, 2H), 7.91 (d, *J* = 7.7 Hz, 2H), 7.42 (ddd, *J* = 8.5, 7.3, 1.3 Hz, 2H), 7.33 (td, *J* = 7.4, 1.0 Hz, 2H), 2.79 (d, *J* = 2.4 Hz, 3H). ^{13}C NMR (101 MHz, $CDCl_3$) δ 170.05, 138.59, 127.32, 126.3, 123.65, 119.81, 116.24, 27.75. MS (EI, m/z): $[M]^+$ calcd for: $C_{14}H_{11}NO$, 209.08; found, 209.05.

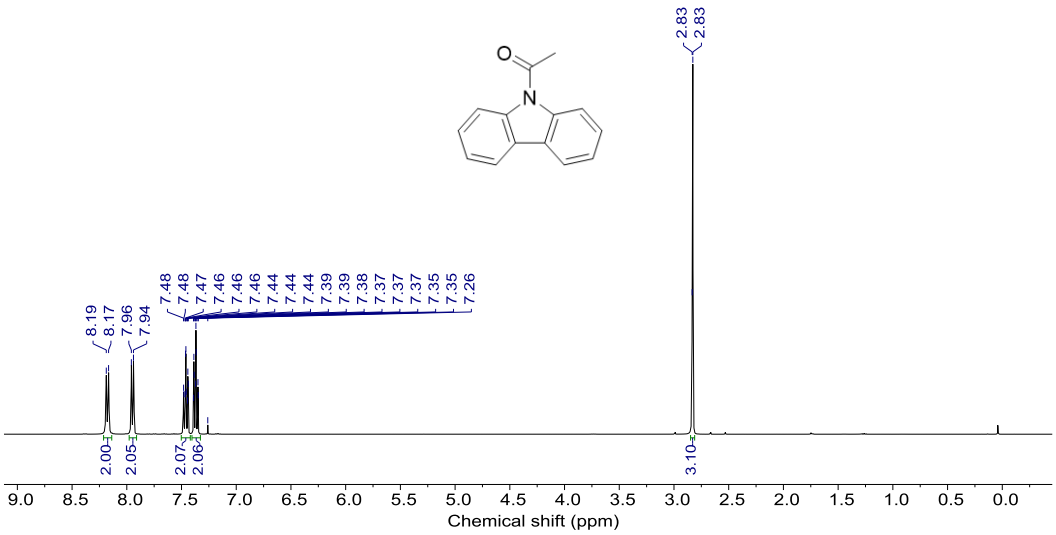

Fig. S1 ^{1}H NMR spectrum of CAC-1 in $CDCl_3$.

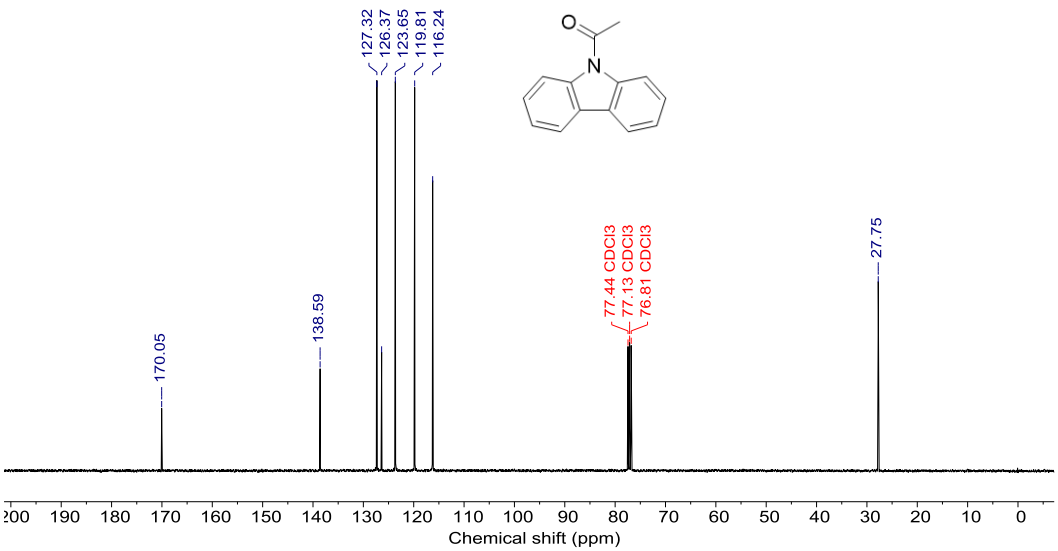

Fig. S2 ^{13}C NMR spectrum of CAC-1 in $CDCl_3$.

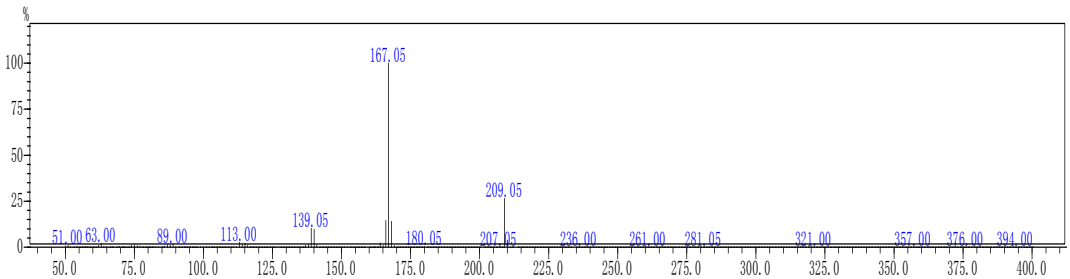

Fig. S3 Gas chromatography-mass (GC-MS) spectrum of CAC-1.

1-(9H-carbazol-9-yl)propan-1-one (CAC-2)

Following the similar synthetic approach for CAC-1, the reaction of carbazole ((1.67 g, 10 mmol), NaH (0.29 g, 12 mmol) and propionyl chloride (1.31 mL, 15 mmol) was conducted to produce CAC-2 (1.11 g, 52.6%) as a white solid.

^{1}H NMR (400 MHz $CDCl_3$) δ 8.20 (d, J = 8.4 Hz, 2H), 7.95 (ddd, J = 7.7, 1.5, 0.7 Hz, 2H), 7.45 (ddd, J = 8.5, 7.3, 1.4 Hz, 2H), 7.35 (td, J = 7.5, 1.0 Hz, 2H), 3.12 (q, J = 7.2 Hz, 2H), 1.40 (t, J = 7.2 Hz, 3H). ^{13}C NMR (101 MHz, $CDCl_3$) δ 173.99, 138.56, 127.30, 126.40, 123.5, 119.78, 116.48, 32.62, 9.02. MS (EI, m/z): $[M]^+$ calcd for: $C_{15}H_{13}NO$, 223.10; found, 233.05.

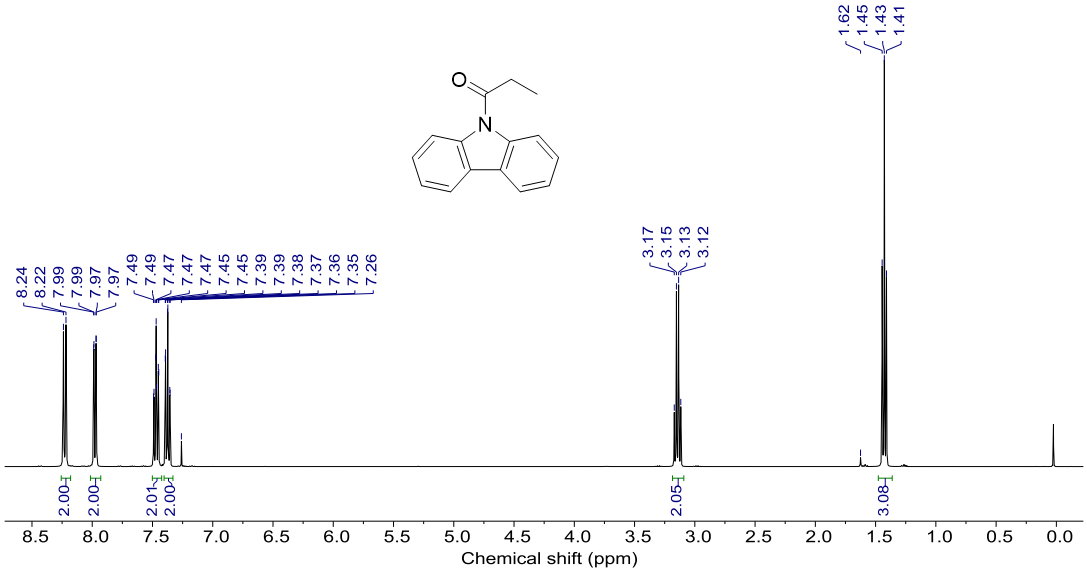

Fig. S4 ^{1}H NMR spectrum of CAC-2 in $CDCl_3$.

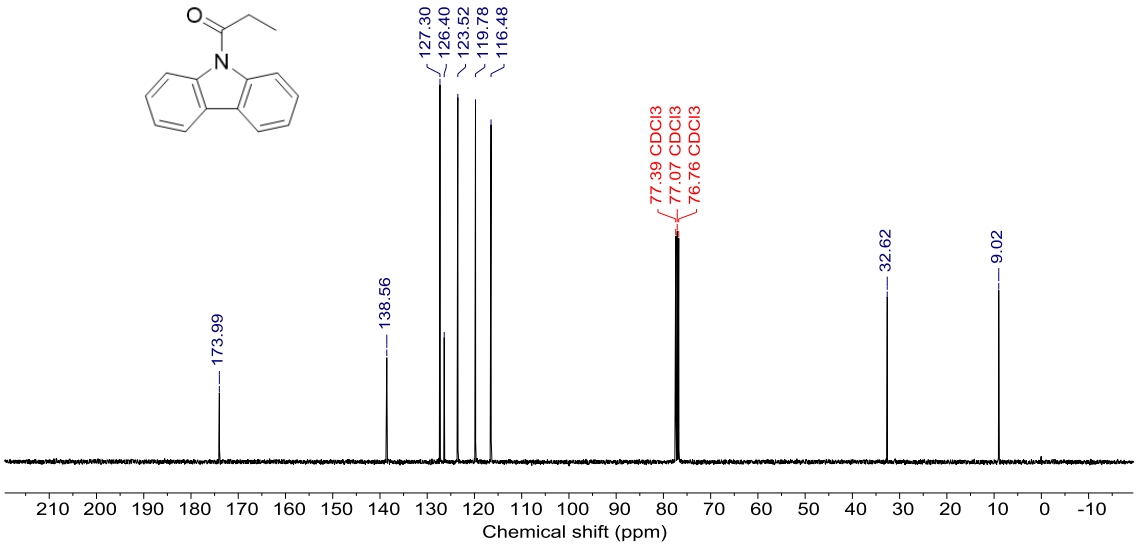

Fig. S5 ^{13}C NMR spectrum of CAC-2 in $CDCl_3$.

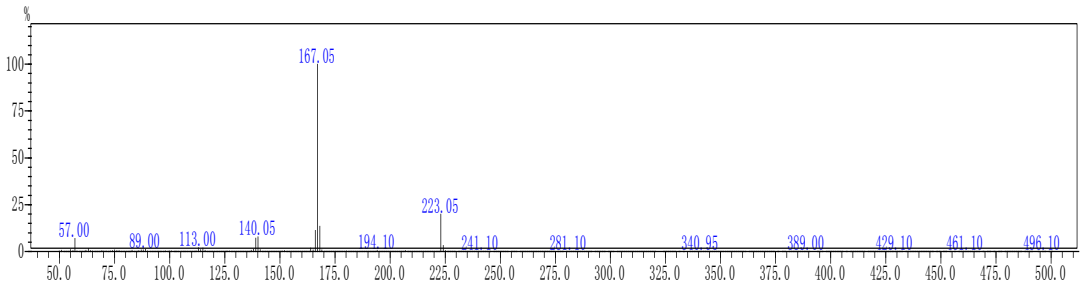

Fig. S6 Gas chromatography-mass (GC-MS) spectrum of CAC-2.

1-(9H-carbazol-9-yl)butan-1-one (CAC-3)

Following the similar synthetic approach for CAC-1, the reaction of carbazole ((1.67 g, 10 mmol), NaH (0.29 g, 12 mmol) and butyryl chloride (1.55 mL, 15 mmol) was conducted to produce CAC-3 (2.18 g, 85.6 %) as a white solid. ^{1}H NMR (400 MHz, $CDCl_3$) δ 8.16 (d, *J* = 8.4 Hz, 2H), 7.91 (d, *J* = 7.6 Hz, 2H), 7.48 – 7.38 (m, 2H), 7.32 (t, *J* = 7.5 Hz, 2H), 3.01 (t, *J* = 7.3 Hz, 2H), 1.93 (p, *J* = 7.4 Hz, 2H), 1.09 (t, *J* = 7.4 Hz, 3H). ^{13}C NMR (101 MHz, $CDCl_3$) δ 173.14, 138.54, 127.26, 126.36, 123.48, 119.76, 116.44, 41.06, 18.15, 13.87. MS (EI, m/z): $[M]^+$ calcd for: $C_{16}H_{15}NO$, 237.21; Found, 237.05.

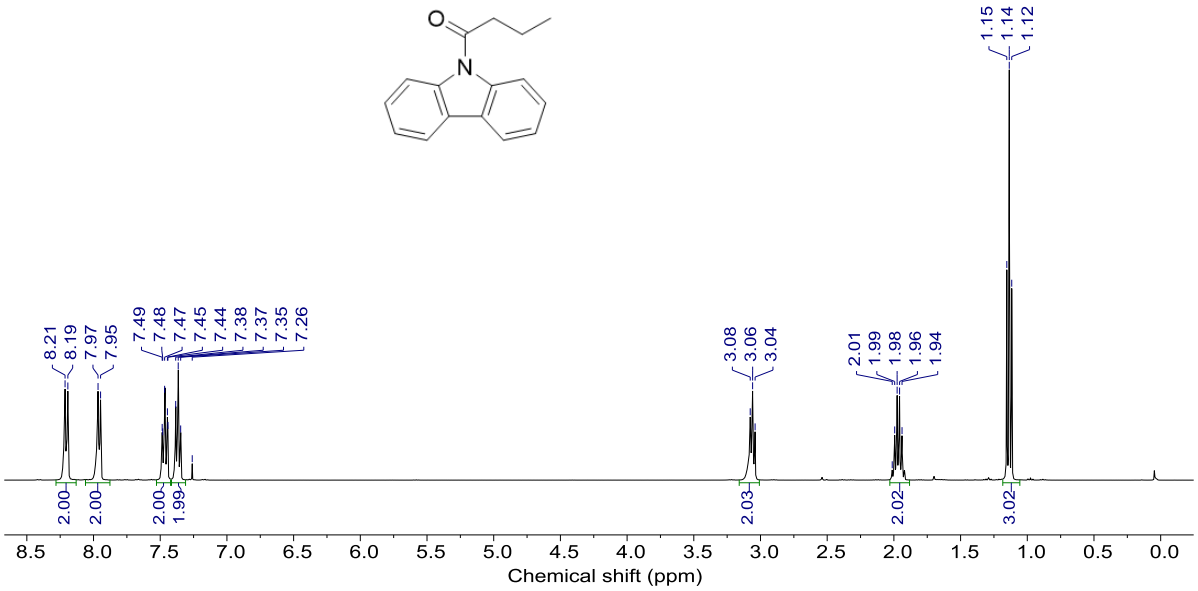

Fig.S7 ^{1}H NMR spectrum of CAC-3 in $CDCl_3$.

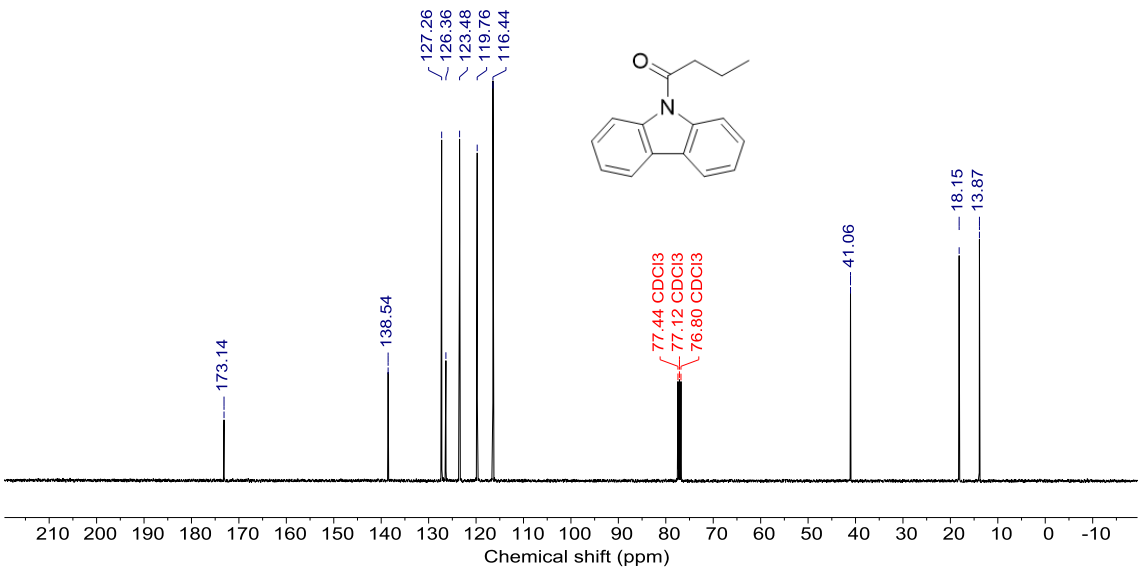

Fig. S8 ^{13}C NMR spectrum of CAC-3 in $CDCl_3$.

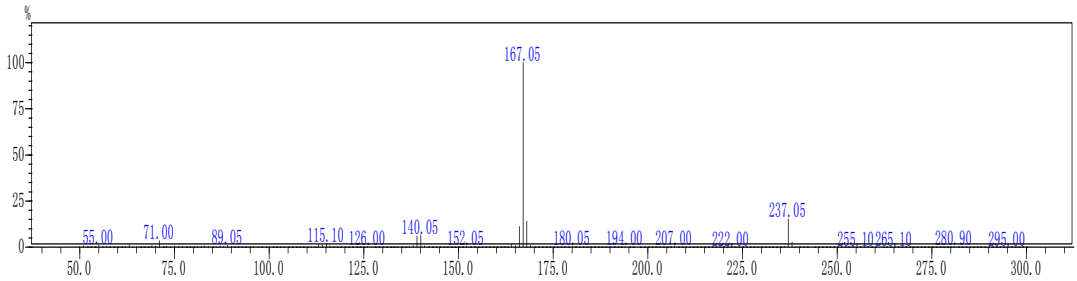

Fig. S9 Gas chromatography-mass (GC-MS) spectrum of CAC-3.

1-(9H-carbazol-9-yl)pentan-1-one (CAC-4)

Following the similar synthetic approach for CAC-1, the reaction of carbazole ((1.67 g, 10 mmol), NaH (0.29 g, 12 mmol) and valeryl chloride (1.78 mL, 15mmol) was conducted to produce CAC-4 (1.50 g, 62.7%) as a white solid. ^{1}H NMR (400 MHz, $CDCl_3$) δ 8.20 (d, *J* = 8.3 Hz, 2H), 7.97 (dd, *J* = 7.7, 0.8 Hz, 2H), 7.46 (ddd, *J* = 8.6, 7.3, 1.4 Hz, 2H), 7.36 (td, *J* = 7.5, 0.9 Hz, 2H), 3.10 (t, *J* = 7.4 Hz, 2H), 1.90 (p, *J* = 7.5 Hz, 2H), 1.52 (dq, *J* = 14.8, 7.4 Hz, 2H), 1.01 (t, *J* = 7.3 Hz, 3H). ^{13}C NMR (101 MHz, $CDCl_3$) δ 173.37, 138.57, 127.29, 126.38, 123.50, 119.79, 116.44, 38.92, 26.77, 22.43, 14.04. MS (EI, m/z): $[M]^+$ calcd for: $C_{17}H_{17}NO$, 251.13; found, 251.10.

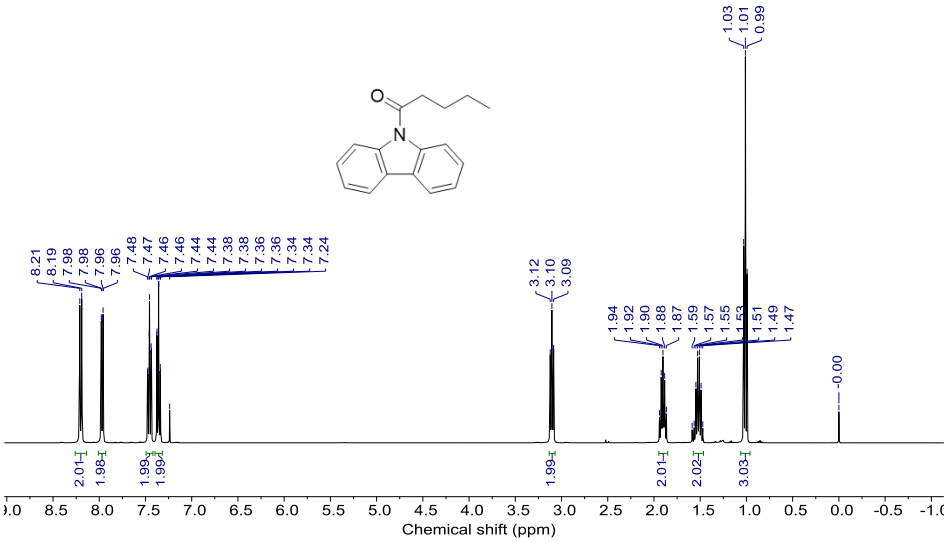

Fig. S10 ^{1}H NMR spectrum of CAC-4 in $CDCl_3$.

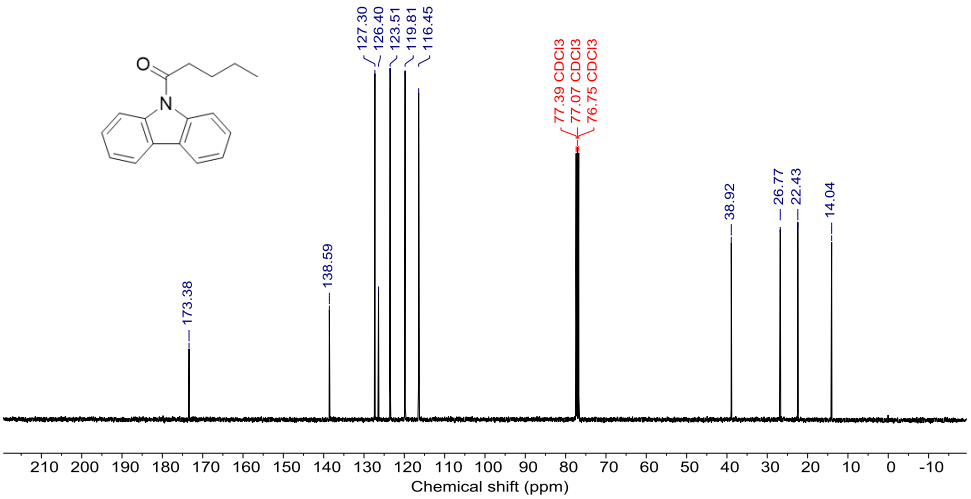

Fig. S11 ^{13}C NMR spectrum of CAC-4 in $CDCl_3$.

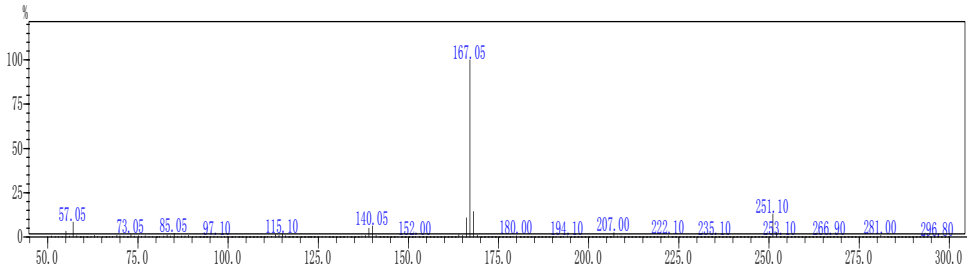

Fig. S12 Gas chromatography-mass (GC-MS) spectrum of CAC-4.

1-(9H-carbazol-9-yl)hexan-1-one (CAC-5)

Following the similar synthetic approach for CAC-1, the reaction of carbazole ((1.67 g, 10 mmol), NaH (0.29 g, 12 mmol) and hexanoyl chloride (1.83 mL, 15 mmol) was conducted to produce CAC-5 (1.40 g, 55.4 %) as a white solid. ^{1}H NMR (400 MHz, $CDCl_3$) δ 8.17 (d, *J* = 8.5 Hz, 2H), 7.93 (d, *J* = 7.8 Hz, 2H), 7.43 (t, *J* = 7.8 Hz, 2H), 7.33 (t, *J* = 7.5 Hz, 2H), 3.04 (t, *J* = 7.4 Hz, 2H), 1.90 (p, *J* = 8.2, 7.6 Hz, 2H), 1.54 – 1.29 (m, 4H), 0.94 (td, *J* = 7.0, 1.7 Hz, 3H). ^{13}C NMR (101 MHz, $CDCl_3$) δ 173.34, 138.56, 127.27, 126.37, 123.48, 119.77, 116.44, 39.18, 31.48, 24.40, 22.65, 14.05. MS (EI, m/z): $[M]^+$ calcd for: $C_{18}H_{19}NO$, 265.15; found, 265.15.

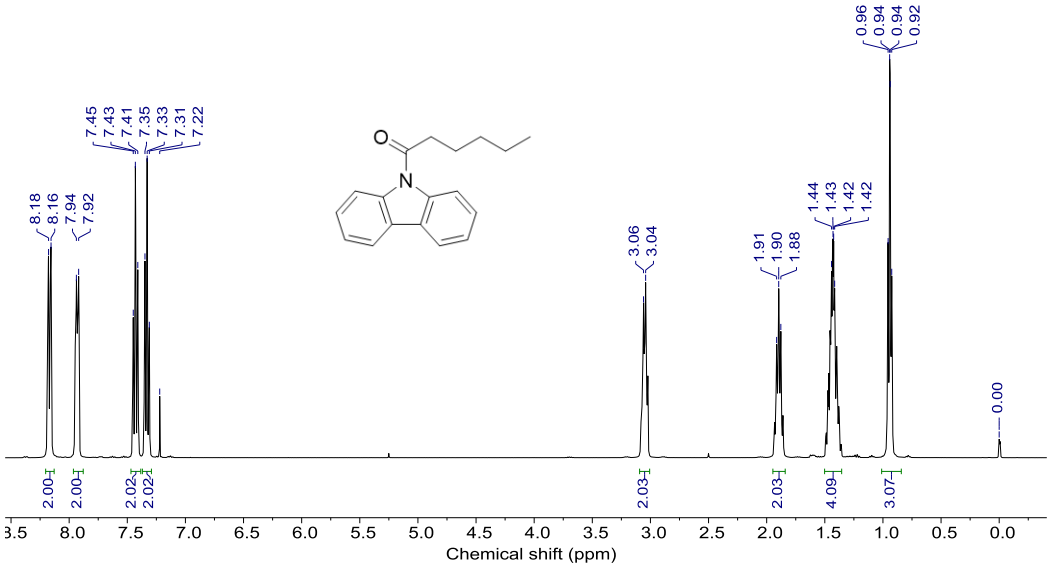

Fig. S13 ^{1}H NMR spectrum of CAC-5 in $CDCl_3$.

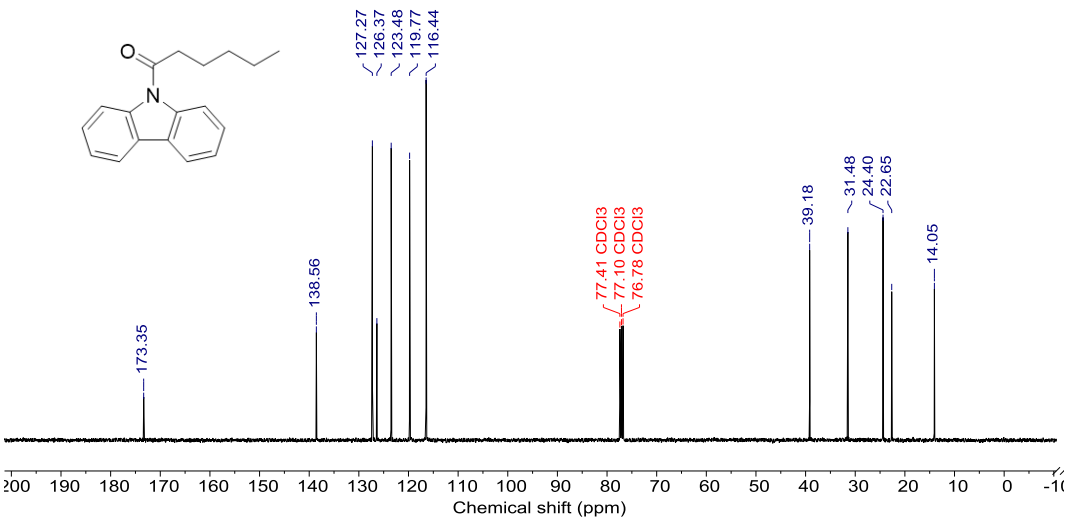

Fig. S14 ^{13}C NMR spectrum of CAC-5 in $CDCl_3$.

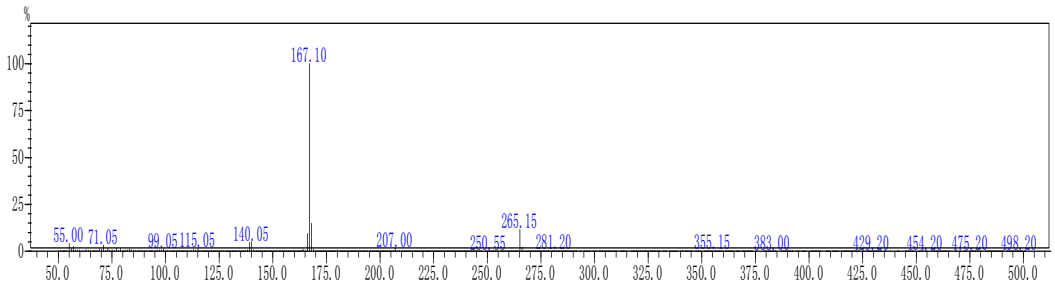

Fig. S15 Gas chromatography-mass (GC-MS) spectrum of CAC-5.

1-(9H-carbazol-9-yl)heptan-1-one) (CAC-6)

Following the similar synthetic approach for CAC-1, the reaction of carbazole ((1.67 g, 10 mmol), NaH (0.29 g, 12 mmol) and heptanoyl chloride (1.83 mL, 15 mmol) was conducted to produce CAC-6 (1.88 g, 67.5 %) as a white solid. ^{1}H NMR (400 MHz, $CDCl_3$) δ 8.20 (d, J = 8.3 Hz, 2H), 7.97 (dd, J = 7.6, 1.4 Hz, 2H), 7.46 (ddd, J = 8.6, 7.3, 1.4 Hz, 2H), 7.36 (td, J = 7.5, 0.9 Hz, 2H), 3.15 – 3.03 (m, 2H), 1.91 (p, J = 7.5 Hz, 2H), 1.49 (t, J = 7.4 Hz, 2H), 1.42 – 1.29 (m, 4H), 0.96 – 0.85 (m, 3H). ^{13}C NMR (101 MHz, $CDCl_3$) δ 173.38, 138.58, 127.29, 126.38, 123.50, 119.79, 116.45, 39.23, 31.74, 29.00, 24.68, 22.59, 14.0. MS (EI, m/z): $[M]^+$ calcd for: $C_{19}H_{21}NO$, 279.16; Found, 279.20.

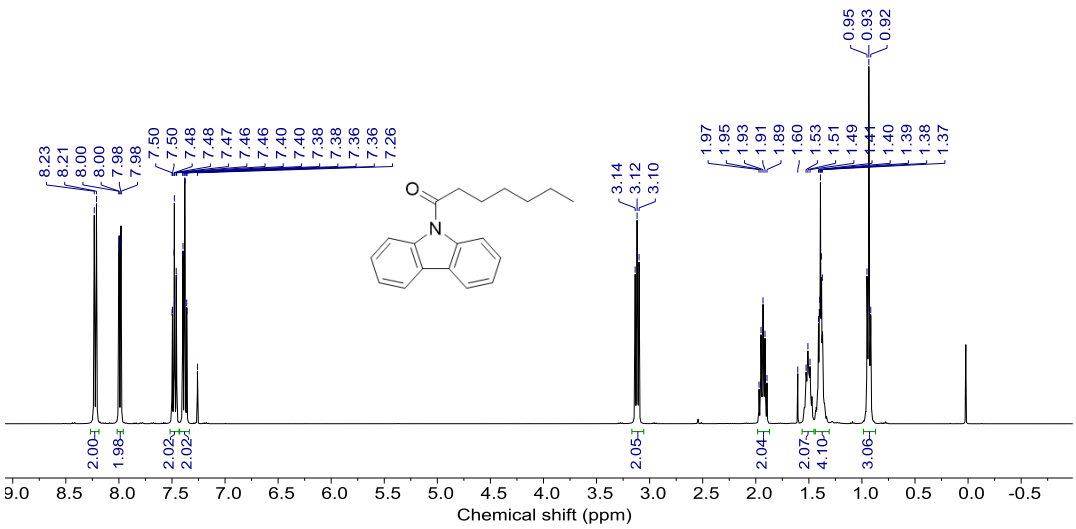

Fig. S16 ^{1}H NMR spectrum of CAC-6 in $CDCl_3$.

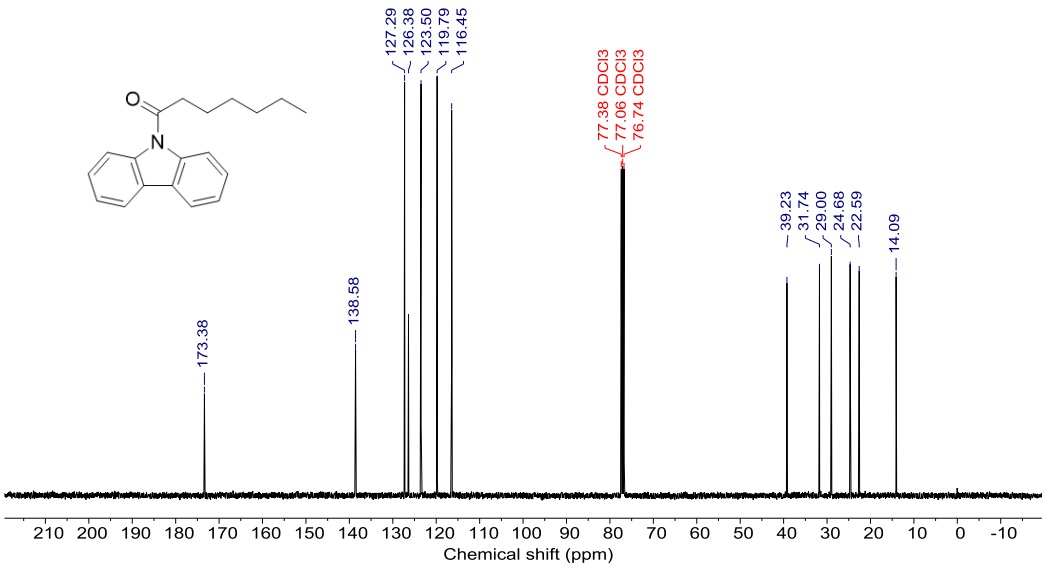

Fig. S17 ^{13}C NMR spectrum of CAC-6 in $CDCl_3$.

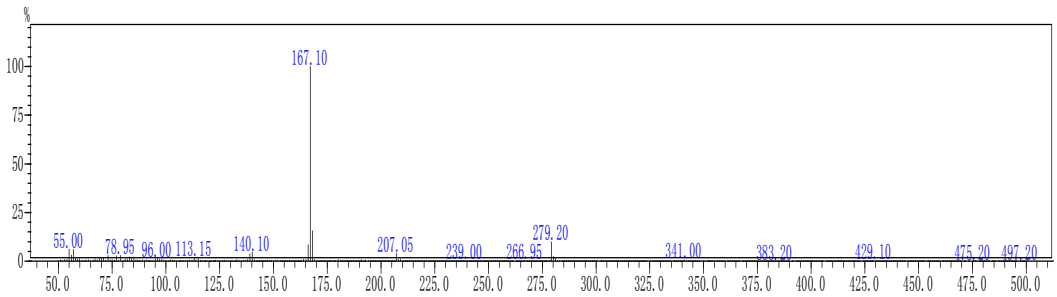

Fig. S18 Gas chromatography-mass (GC-MS) spectrum of CAC-6.

1-(9H-carbazol-9-yl)octan-1-one (CAC-7)

Following the similar synthetic approach for CAC-1, the reaction of carbazole ((1.67 g, 10 mmol), NaH (0.29 g, 12 mmol) and octanoyl chloride (1.83 mL, 15 mmol) was conducted to produce CAC-7 (2.08 g, 71.05 %) as a white solid. ^{1}H NMR (400 MHz, Chloroform-*d*) δ 8.23 (d, *J* = 8.4 Hz, 2H), 8.01 (s, 2H), 7.52 – 7.45 (m, 2H), 7.38 (t, *J* = 7.4 Hz, 2H), 3.13 (t, *J* = 7.3 Hz, 2H), 1.94 (p, *J* = 7.4 Hz, 2H), 1.55-1.29 (m, 9H), 0.91 (t, *J* = 6.6 Hz, 3H).^{13}C NMR (101 MHz, Chloroform-*d*) δ 173.41, 138.60, 127.30, 126.40, 123.51, 119.80, 116.45, 39.23, 31.74, 29.28, 29.22, 24.72, 22.66, 14.11. MS (EI, m/z): $[M]^+$ calcd for: $C_{20}H_{23}NO$, 293.18; found, 293.20.

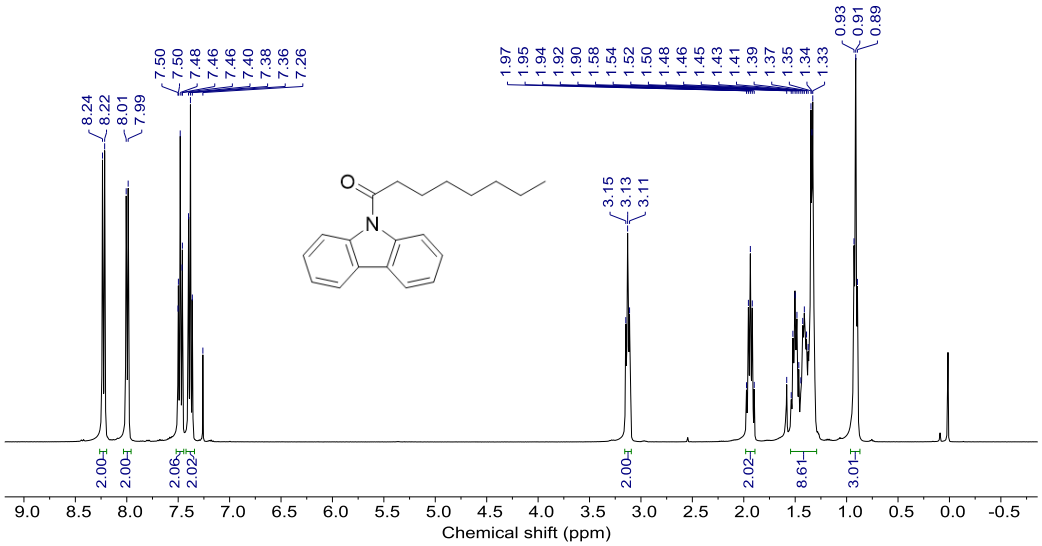

Fig. S19 ^{1}H-NMR spectrum of CAC-7 in $CDCl_3$.

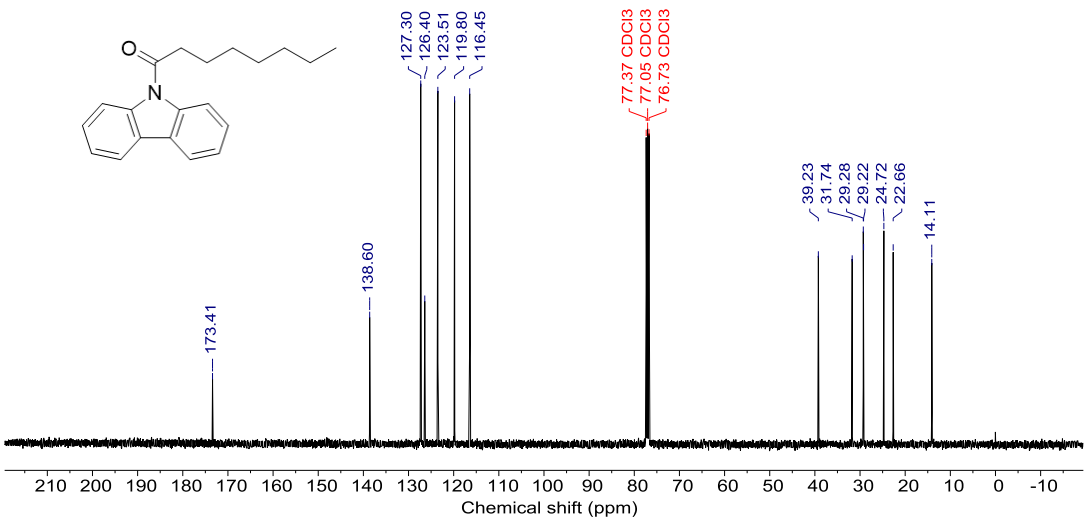

Fig. S20 ^{13}C NMR spectrum of CAC-7 in $CDCl_3$.

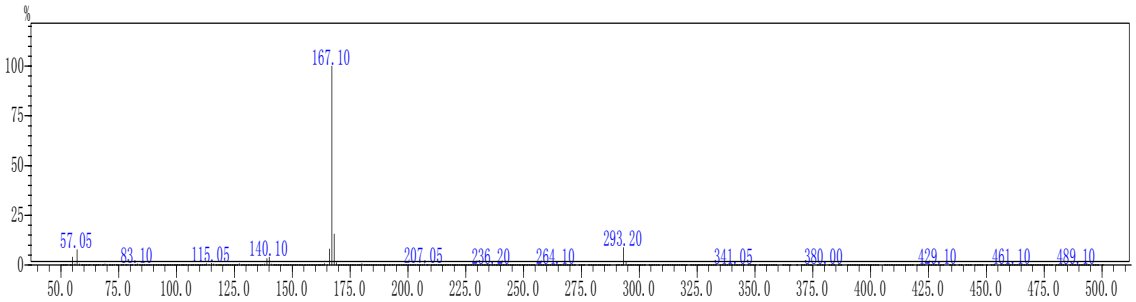

Fig. S21 Gas chromatography-mass (GC-MS) spectrum of CAC-7.

1-(9H-carbazol-9-yl)nonan-1-one (CAC-8)

Following the similar synthetic approach for CAC-1, the reaction of carbazole ((1.67 g, 10 mmol), NaH (0.29 g, 12 mmol) and nonanoyl chloride (2.79 mL, 15 mmol) was conducted to produce CAC-8 (2.37 g, 77.2 %) as a white solid. 1-(9H-carbazol-9-yl)nonan-1-one: ^{1}H NMR (400 MHz, Chloroform-*d*) δ 8.23 (d, *J* = 8.4 Hz, 2H), 8.00 (dd, *J* = 7.7, 1.3 Hz, 2H), 7.51 – 7.45 (m, 2H), 7.38 (t, *J* = 7.4 Hz, 2H), 3.14 (t, *J* = 7.4 Hz, 2H), 1.94 (p, *J* = 7.5 Hz, 2H), 1.54 – 1.27 (m, 11H), 0.90 (t, *J* = 6.6 Hz, 3H). ^{13}C NMR (101 MHz, Chloroform-*d*) δ 173.42, 138.61, 127.30, 126.41, 123.51, 119.81, 116.46, 39.24, 31.85, 29.50, 29.31, 29.20, 24.72, 22.69, 14.13. MS (EI, m/z): $[M]^{+}$ calcd for: $C_{21}H_{25}NO$, 307.19; found, 307.15.

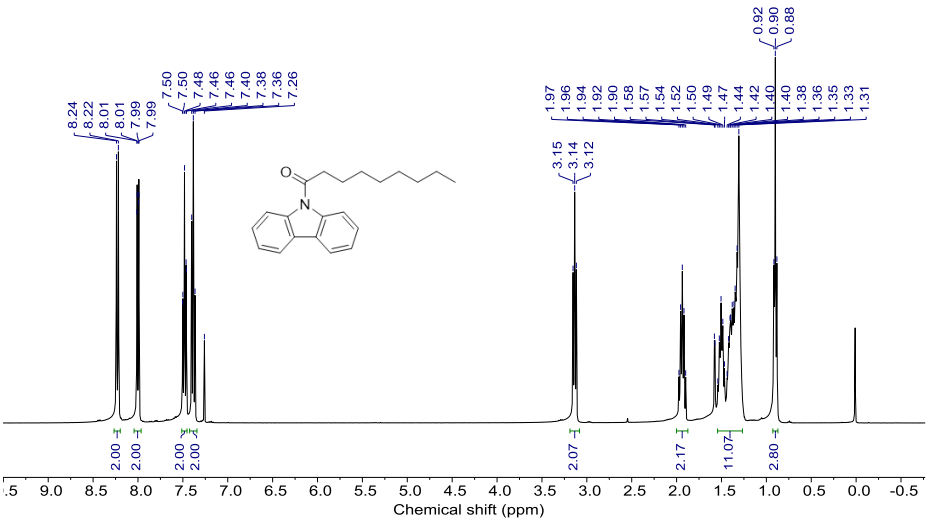

Fig. S22 ^{1}H NMR spectrum of CAC-8 in $CDCl_3$.

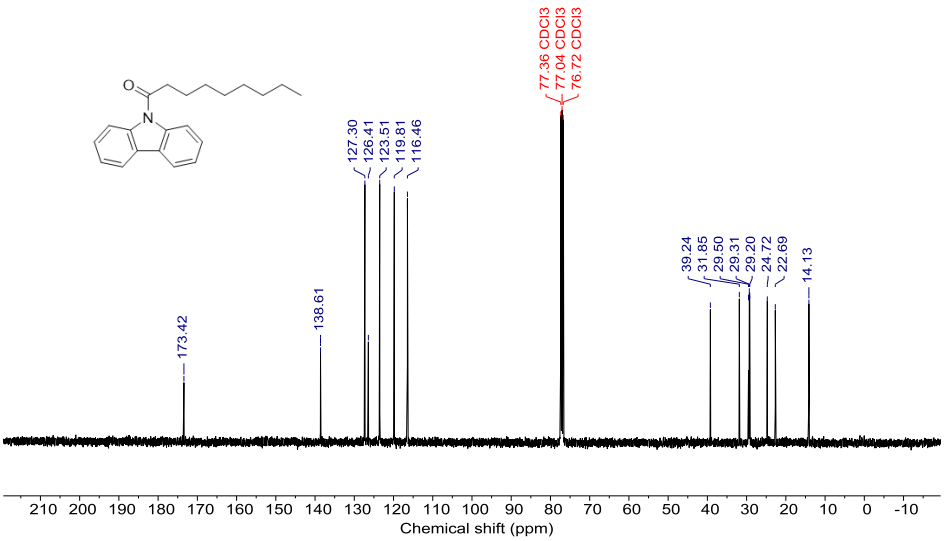

Fig. S23 ^{13}C NMR spectrum of CAC-8 in $CDCl_3$.

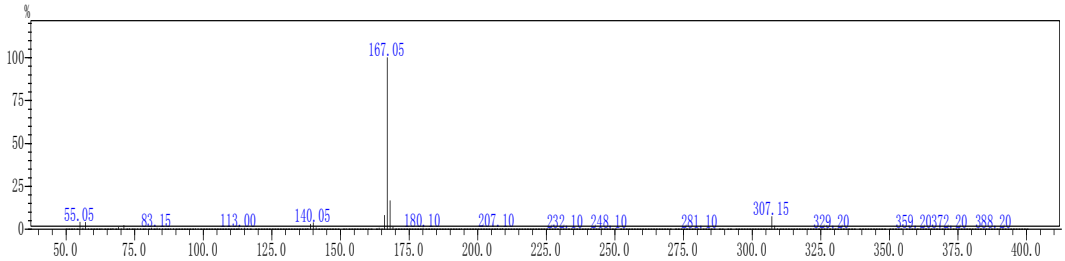

Fig. S24 Gas chromatography-mass (GC-MS) spectrum of CAC-8.

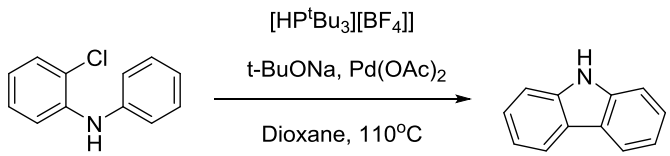

Scheme S2. Synthetic route of lab-carbazole.

Lab-carbazole (L-Cz)

2-Chloro-N-phenylaniline (7.5 g, 36.8 mmol), t-BuONa (17.68 g, 184 mmol), $Pd(OAc)_2$ (0.2 g, 1.0 mmol), and HP^tBu_3•BF_4 (0.53 g,1.8 mmol) were suspended in dioxane (200 mL) under the protection of nitrogen. The mixture was heated to reflux (110 ^oC) for 18 h under magnetic stirring before quenched by addition of HCl (aq) (2 M, 20 mL). The organic phase was extracted with CH_2Cl_2 (3 × 40 mL), and removed by rotatory evaporation after dried over by Na_2SO_4. The crude product was purified by column chromatography with petroleum ether and dichloromethane as eluent (V/V, 10/1), followed by recrystallized in toluene several times to give pure product as a pure white solid with 1.52 g. ^{1}H NMR (400 MHz, DMSO-d_6) δ 11.25 (s, 1H), 8.13 – 8.08 (m, 2H), 7.48 (dt, J = 8.1, 0.9 Hz, 2H), 7.37 (ddd, J = 8.2, 7.1, 1.2 Hz, 2H), 7.15 (ddd, J = 8.0, 7.1, 1.0 Hz, 2H).

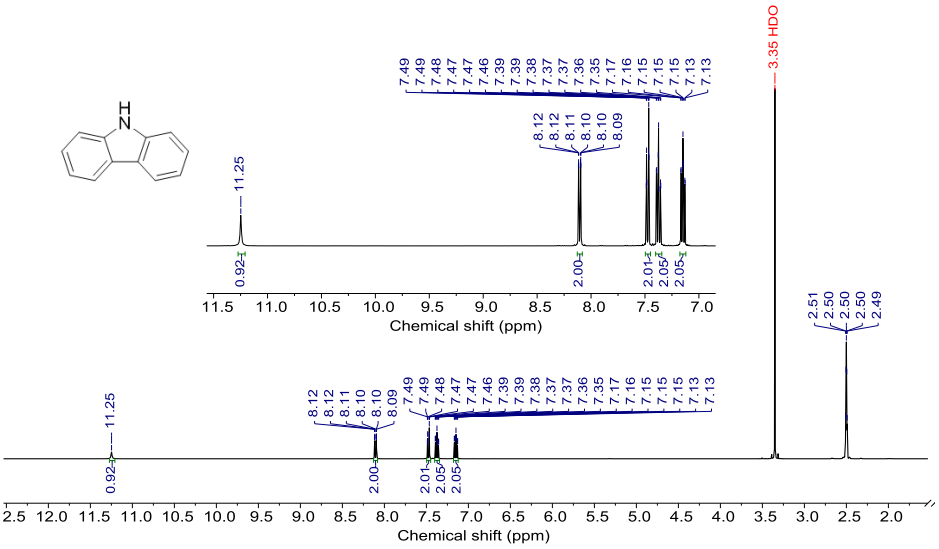

Fig. S25 ^{1}H NMR spectrum of lab-carbazole in DMSO-d_6.

Supplementary Figures and Tables

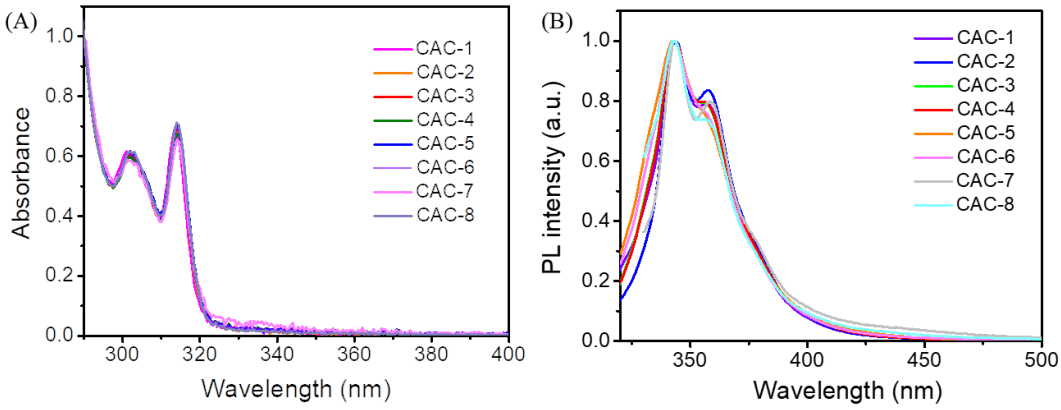

Fig. S26 The UV-vis absorption (A) and PL (B) spectra of CAC-*N* (*N* = 1 ~ 8) in dilute THF solution (c = 1.0×10^{-5} M), λ_{Ex} = 310 nm.

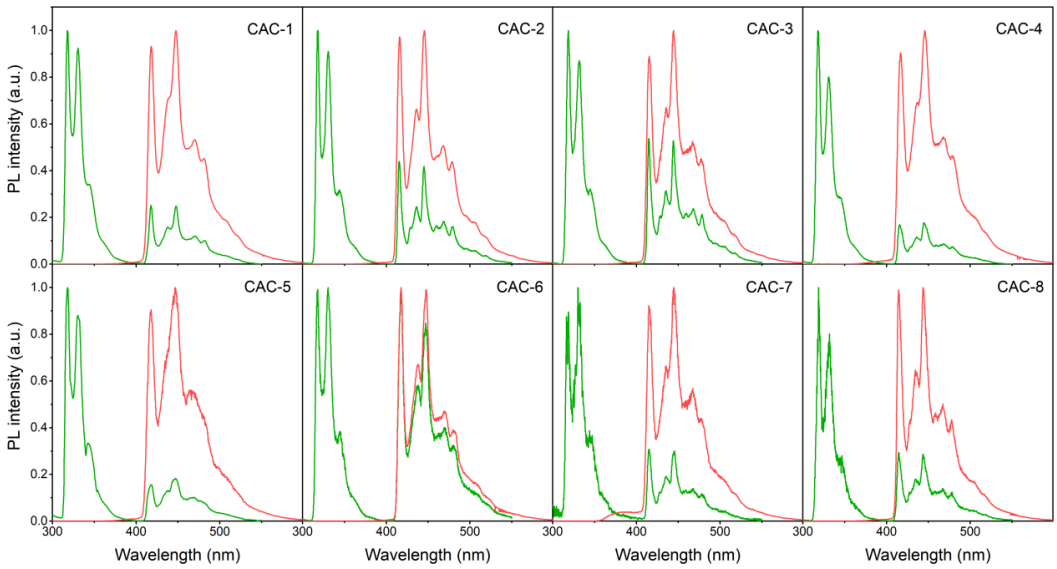

Fig. S27 The PL (green line) and phosphorescence (red line) spectra of CAC-*N* (*N* = 1 ~ 8) in dilute THF solution (c = 1.0×10^{-5} M) under 77 K, λ_{Ex} = 289 nm.

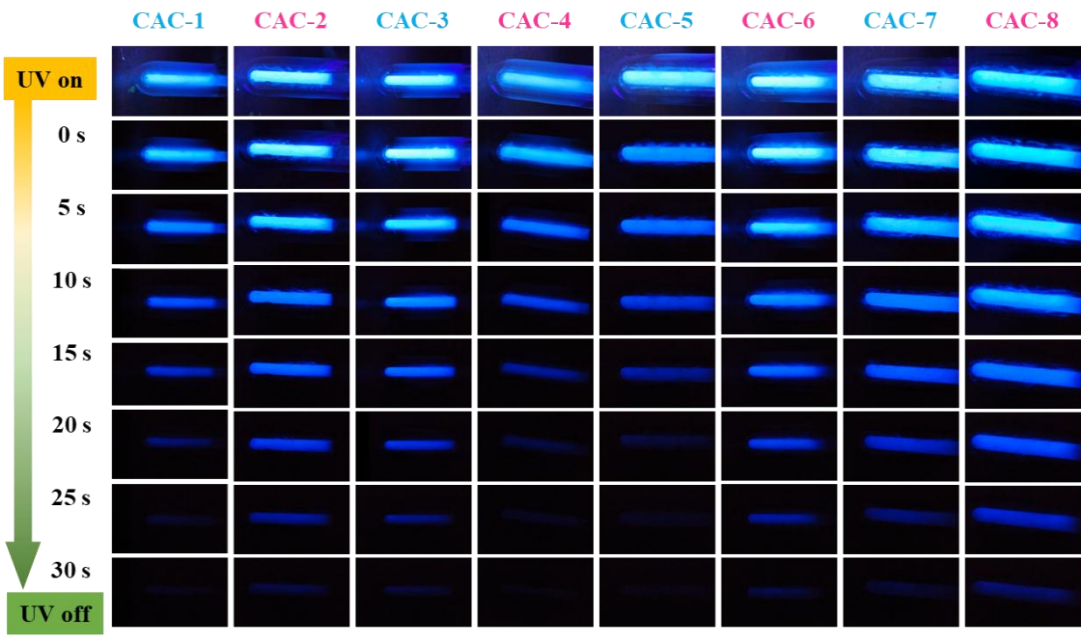

Fig. S28 The photographs of eight compounds in THF solution under 77 K of liquid nitrogen, upon 365 nm UV on and UV off after 0, 5, 10, 15, 20, 25, and 30 s.

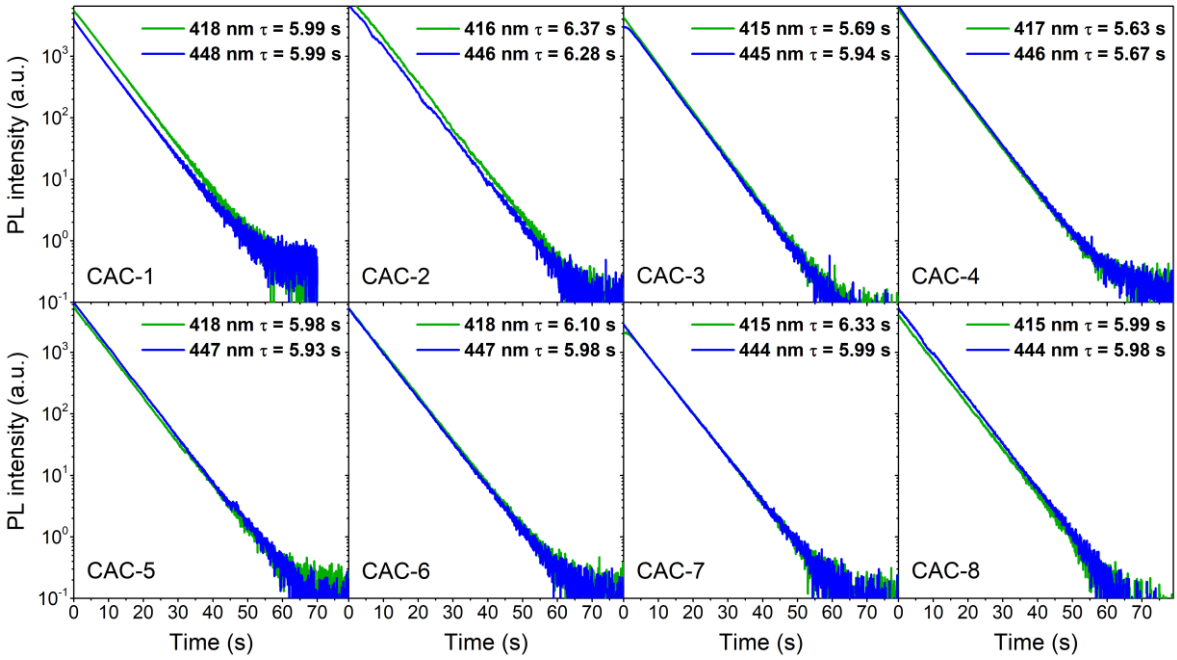

Fig. S29 Time-resolved phosphorescence decay profiles of CAC-*N* (*N* = 1 ~ 8) in dilute THF solution under 77 K, λ_{Ex} = 289 nm.

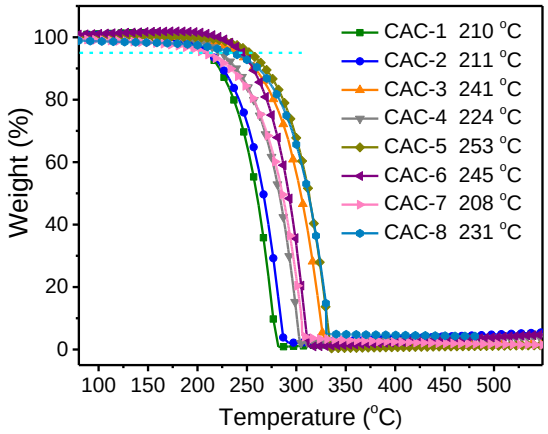

Fig. S30 TGA curves of eight compounds. The samples were heated at a rate of 20 K min^{-1} in atmosphere of N_2.

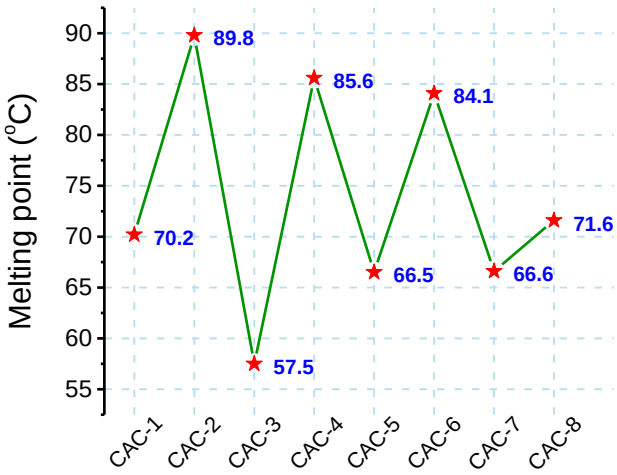

Fig. S31 Schematic presentation of the melting point of these compounds.

Table S1. Unit cell parameters of eight single crystals.

Name	**CAC-1**	**CAC-2**	**CAC-3**	**CAC-4**	**CAC-5**	**CAC-6**	**CAC-7**	**CAC-8**
Formula	$C_{14}H_{11}NO$	$C_{15}H_{13}NO$	$C_{16}H_{15}NO$	$C_{17}H_{17}NO$	$C_{18}H_{19}NO$	$C_{19}H_{21}NO$	$C_{20}H_{23}NO$	$C_{21}H_{25}NO$
CCDC	2050872	2050873	2050874	2050875	2050876	2050877	2050878	2050879
Symmetry	Centrosymmetric	Centrosymmetric	Centrosymmetric	Noncentrosymmetric	Centrosymmetric	Noncentrosymmetric	Centrosymmetric	Noncentrosymmetric
Crystal system	monoclinic	orthorhombic	orthorhombic	orthorhombic	orthorhombic	orthorhombic	monoclinic	orthorhombic
Space Group	I2/a	Pbca	Pbca	$Pna2_1$	Pccn	$Pna2_1$	$P2_1/c$	$Pna2_1$
Cell Length (Å)	a 17.5197(5) b 4.36700(10) c 55.732(2)	a 8.94349(19) b 15.3282(3) c 16.5685(4)	a 8.83939(11) b 15.1885(2) c 18.7093(2)	a 5.97062(8) b 24.9105(4) c 9.11019(17)	a 24.8983(2) b 16.9181(2) c 6.91920(10)	a 5.80290(10) b 29.1697(4) c 9.1710(2)	a 9.1532(2) b 31.2312(5) c 5.75440(10)	a 5.75150(10) b 32.9639(5) c 9.1867(2)
Cell Angle (^{0})	α 90.00 β 91.514(3) γ 90.00	α 90.00 β 90.00 γ 90.00	α 90.00 β 90.00 γ 90.00	α 90.00 β 90.00 γ 90.00	α 90.00 β 90.00 γ 90.00	α 90.00 β 90.00 γ 90.00	α 90.00 β 91.535(2) γ 90.00	α 90.00 β 90.00 γ 90.00
Cell Volume ($Å^3$)	4262.5(2)	2271.33(8)	2511.85(5)	1354.97(4)	2914.59(6)	1552.36(5)	1644.39(5)	1741.72
Z	16	7	8	4	8	4	4	4
Density (g/cm^3)	1.304	1.143	1.2549	1.2319	1.2094	1.1953	1.185	1.172
F(000)	1760.0	826.0	1011.0	537.6	1139.3	601.7	632.0	664.0
h_{max}, k_{max}, l_{max}	20, 5, 66	7, 17, 18	10, 18, 22	7, 29, 9	29, 20, 8	6, 34, 10	10, 37, 6	6, 39, 10

Table S2. The melting point (T_m), fluorescence (λ_{PL}) and corresponding lifetime (τ), PLQY (Φ_{PL}), RTP (λ_{RTP}) and corresponding lifetime.

Compounds	**CAC-1**	**CAC-2**	**CAC-3**	**CAC-4**	**CAC-5**	**CAC-6**	**CAC-7**	**CAC-8**
T_m (^{o}C)	70.2	89.8	57.5	85.6	66.5	84.1	66.6	71.6
λ_{PL} (nm) / τ (ns)	386 / 9.44	370 / 9.19	388 / 6.81	389 / 10.40	349 / 5.29	355 / 5.39	352 / 11.93	350 / 6.51
Φ_{PL} (%)	24.18	42.26	6.11	19.04	29.00	25.12	17.92	8.57
λ_{ML} (nm)	×	×	×	370	×	354	×	348
λ_{RTP} (nm) /τ (ns)	471 / 0.10 560 / 0.27 600 / 0.29	374 / 0.40 390 / 0.33 529 / 0.71 573 / 0.70	531 / 0.80 575 / 0.87	529 / 1.27 572 / 1.26	576 / 0.06	371 / 0.48 389 / 0.49 529 / 1.04 573 / 1.10	×	×

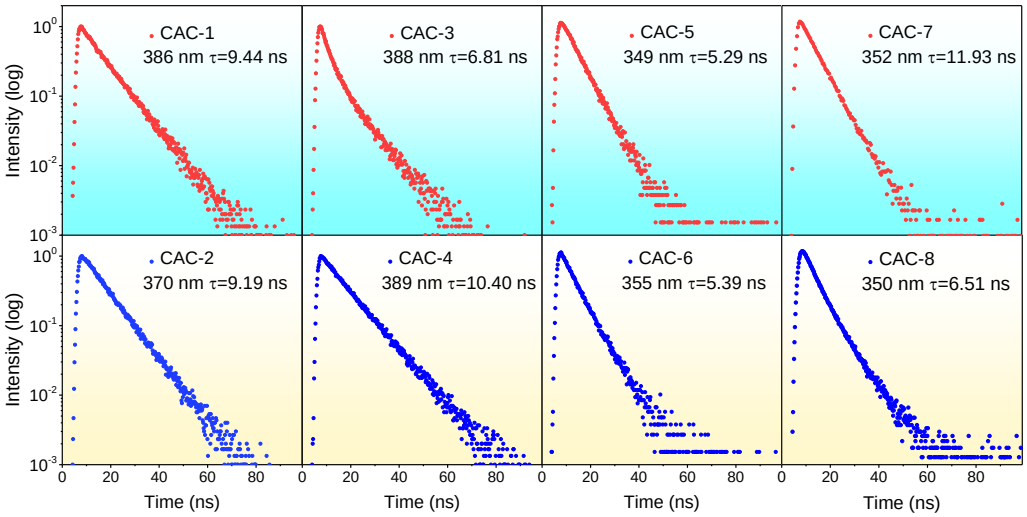

Fig. S32 Time-resolved PL decay profiles of CAC-*N* (*N* = 1~8) crystals under 298 K, λ_{Ex}=310 nm.

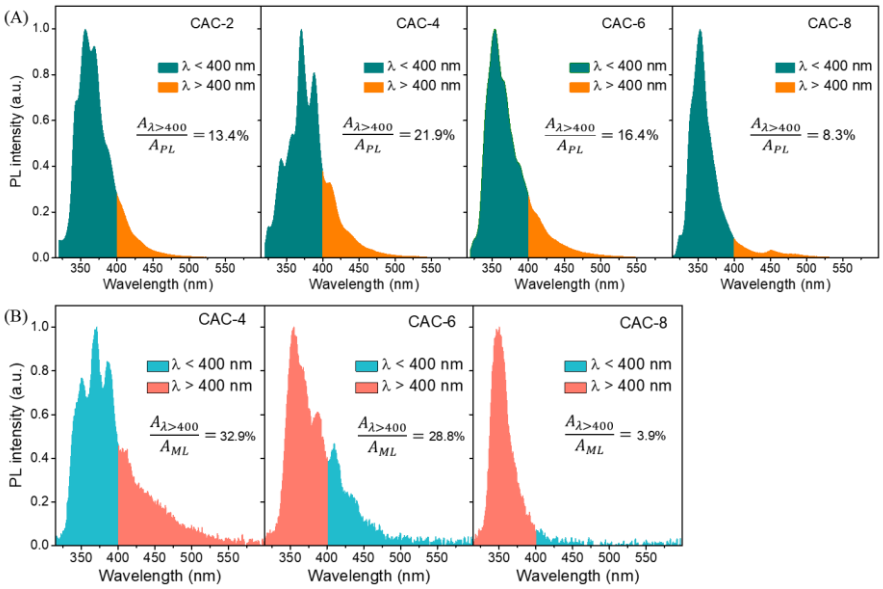

Fig. S33 (A) In the PL of CAC-2, CAC-4, CAC-6 and CAC-8 crystals, the visible emission (λ > 400 nm) area is account for 13.4%, 21.9%, 16.4% and 8.3%; (B) in ML of CAC-4, CAC-6 and CAC-8 crystals, the visible emission area is account for 32.9%, 28.8% and 3.9%. The emission with wavelength larger than 400 nm is defined as visible emission. The proportion of visible emission is calculated as visible emission peak area ($A_{\lambda > 400}$) versus the total spectrum peak area (A_{PL}, A_{ML}), which is calculated by Origin program (version 2016).

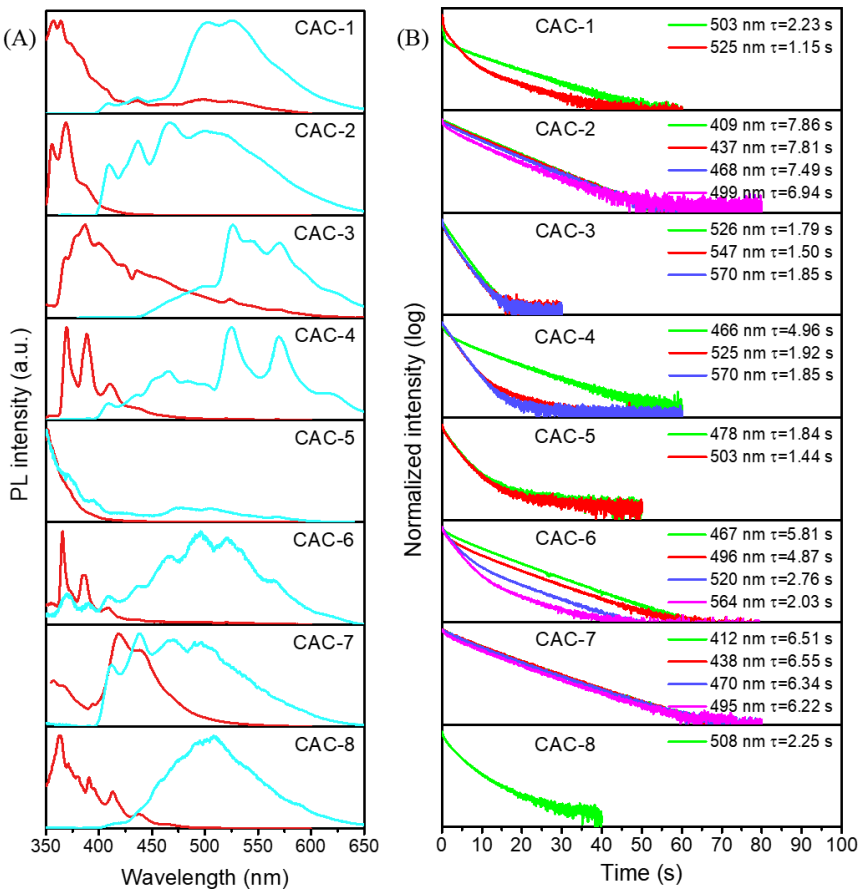

Fig. S34 (A) PL (red line) and phosphorescence (cyan line) spectra of CAC-*N* (*N* = 1 ~ 8) crystals at 77 K; (B) time-resolved phosphorescence decay curves at different emission wavelength.

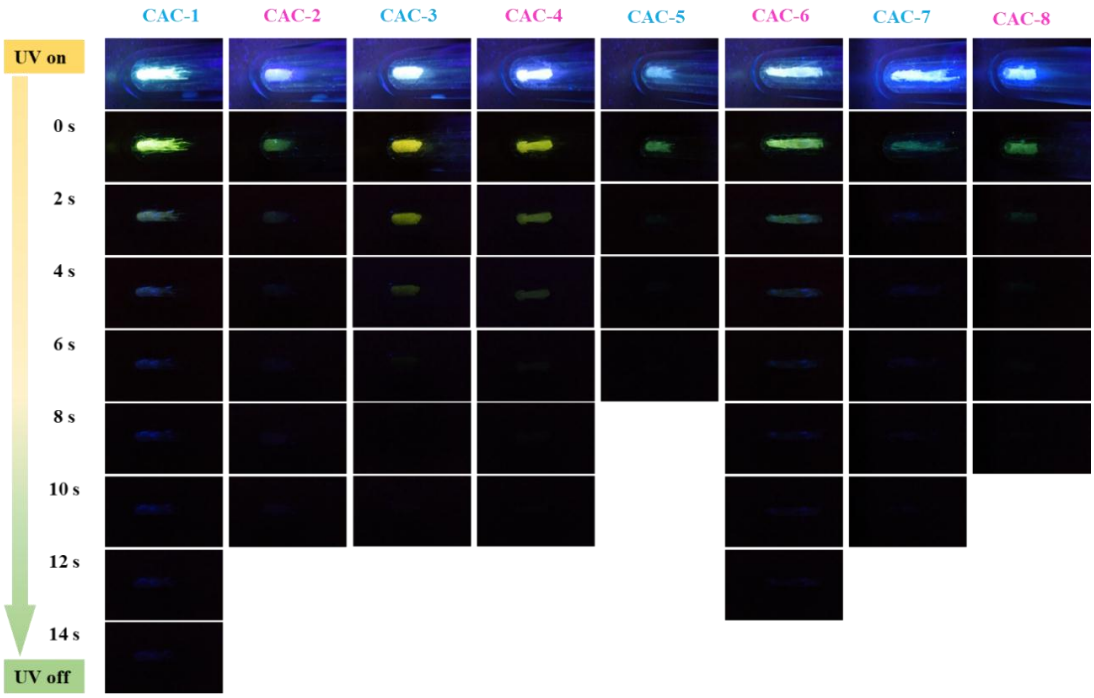

Fig. S35 The photographs of eight crystals under 77 K of liquid nitrogen, upon 365 nm UV on and UV off after 0, 2, 4, 6, 8, 10, 12, and 14 s.

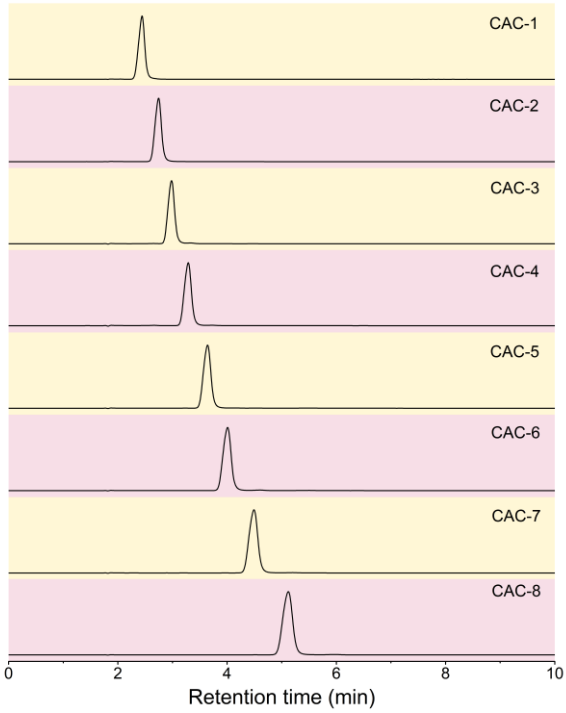

Fig. S36 HPLC spectra of CAC-*N* (*N* = 1 ~ 8) monitored at 254 nm with methanol as eluent at flow rate of 1 mL min^{-1}. A BaseLine C18 column (4.6 × 250 mm, 5.0 μm particles size) was used for chromatographic separation at 40 ^{o}C.

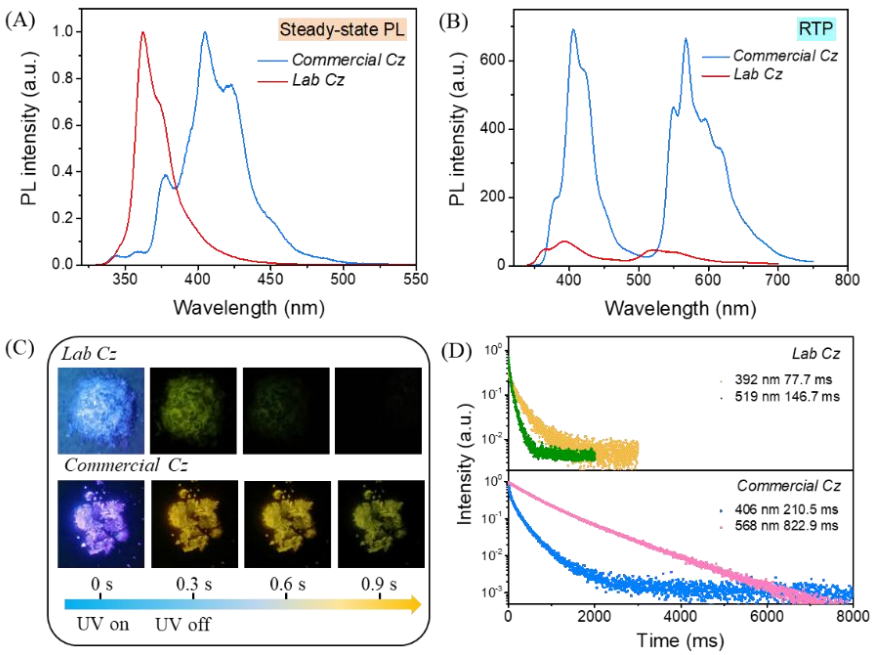

Fig. S37 (A) Steady-state PL spectra of commercial carbazole (Cz) (blue line) and lab carbazole (red line); (B) RTP (green line) spectra of commercial carbazole (blue line) and lab carbazole (red line); (C) photographs of commercial carbazole and lab carbazole, upon 365 nm UV on and UV off after 0.3, 0.6, 0.9 s; (D) time-resolved phosphorescence decay curves at different emission wavelength.

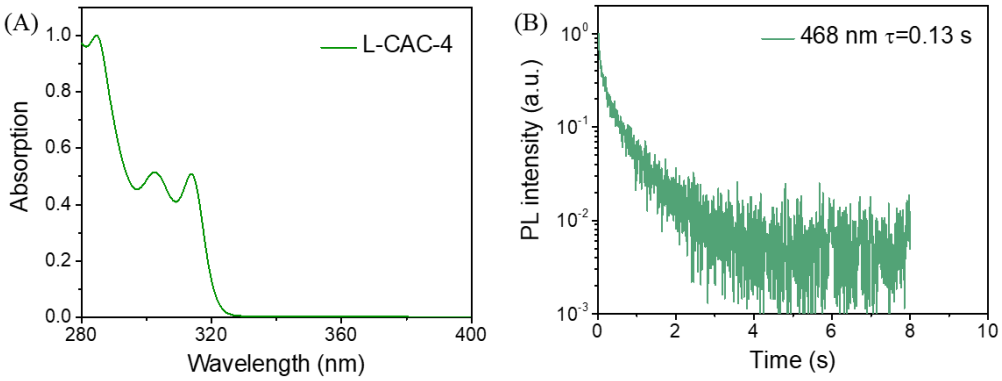

Fig. S38 (A) The absorption spectrum of lab carbazole synthesized CAC-4 (L-CAC-4); (B) time-resolved phosphorescence decay curves at 468 nm under ambient condition, λ_{Ex} = 352 nm.

Table S3. The unit cell parameters of single CAC-4 and L-CAC-4 crystals.

Crystal	CAC-4	L-CAC-4
Formula	$C_{17}H_{17}NO$	$C_{17}H_{17}NO$
Symmetry	Noncentrosymmetric	Noncentrosymmetric
Crystal system	orthorhombic	orthorhombic
Space Group	$Pna2_1$	$Pna2_1$
Cell Length (Å)	a 5.97062(8) b 24.9105(4) c 9.11019(17)	a 5.9682(3) b 24.9107(12) c 9.1101(5)
Cell Angle (^{0})	α 90.00 β 90.00 γ 90.00	α 90.00 β 90.00 γ 90.00
Cell Volume (Å^3)	1354.97(4)	1354.42(12)
Z	4	4
Density (g/cm^3)	1.2319	1.242
F (000)	537.6	544
hmax, k_{max}, l_{max}	7, 29, 9	4, 29, 10

L-CAC-4 is derived from lab synthesized carbazole

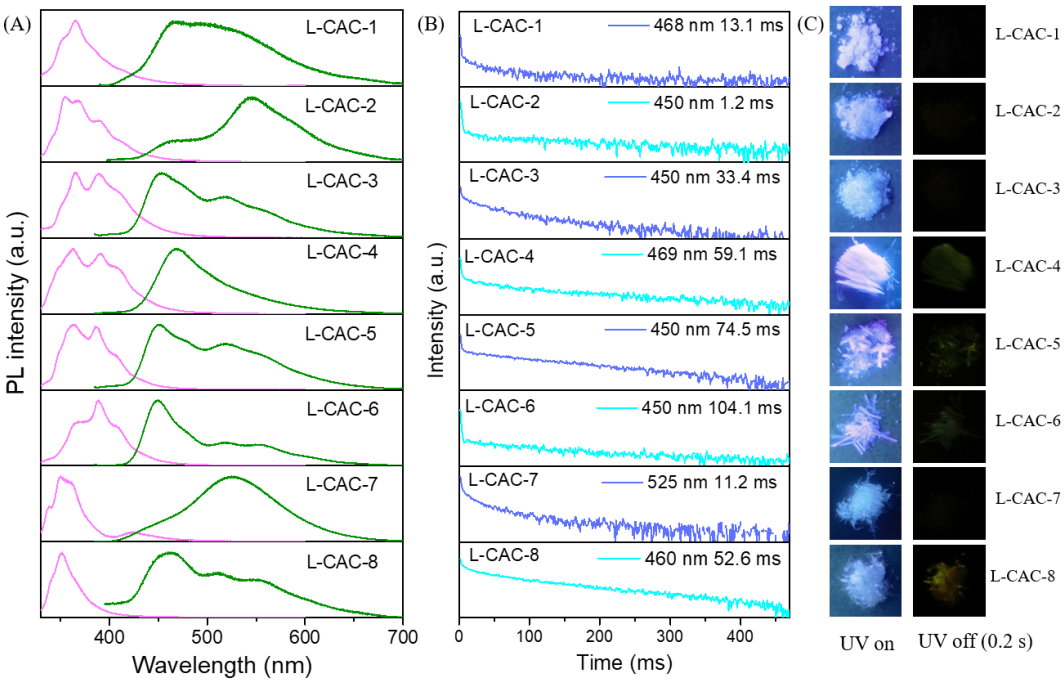

Fig. S39 (A) PL (pink line) (λ_{Ex} = 310 nm) and phosphorescence (green line) (λ_{Ex} = 365 nm) spectra of L-CAC-*N* (*N* = 1 ~ 8) crystals; (B) time-resolved phosphorescence decay curves at different emission wavelength, λ_{Ex} = 365 nm; (C) photographs of eight crystals, upon 365 nm UV on and UV off after 0.2 s.

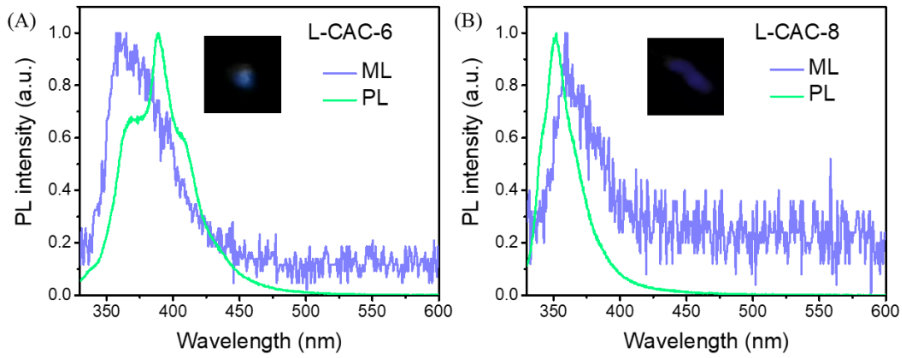

Fig. S40 (A) The PL (green line), ML (purple line) spectra of Lab CAC-6 crystals; (B) PL (green line), ML (purple line) spectra of Lab CAC-8 crystals.

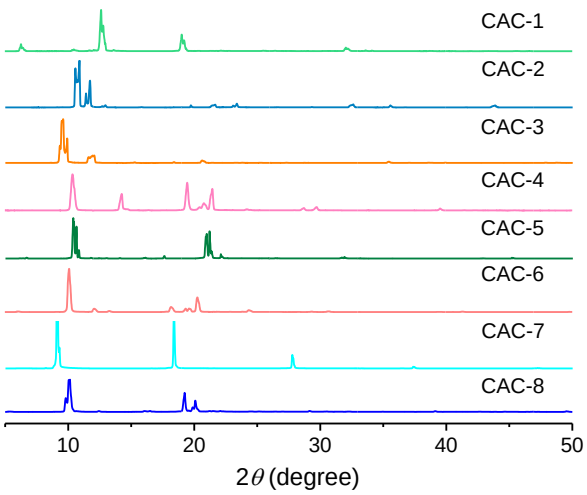

Figure S41. XRD pattern of CAC-*N* (*N* = 1~8) crystals.

Table S4. The unit cell of eight crystals with dimension of 2 × 2 × 2, the carbazole units were separated by the stacked alkyl chains in CAC-4~8. Molecular arrangement can be clearly divided to alkyl zone and aromatic zone.

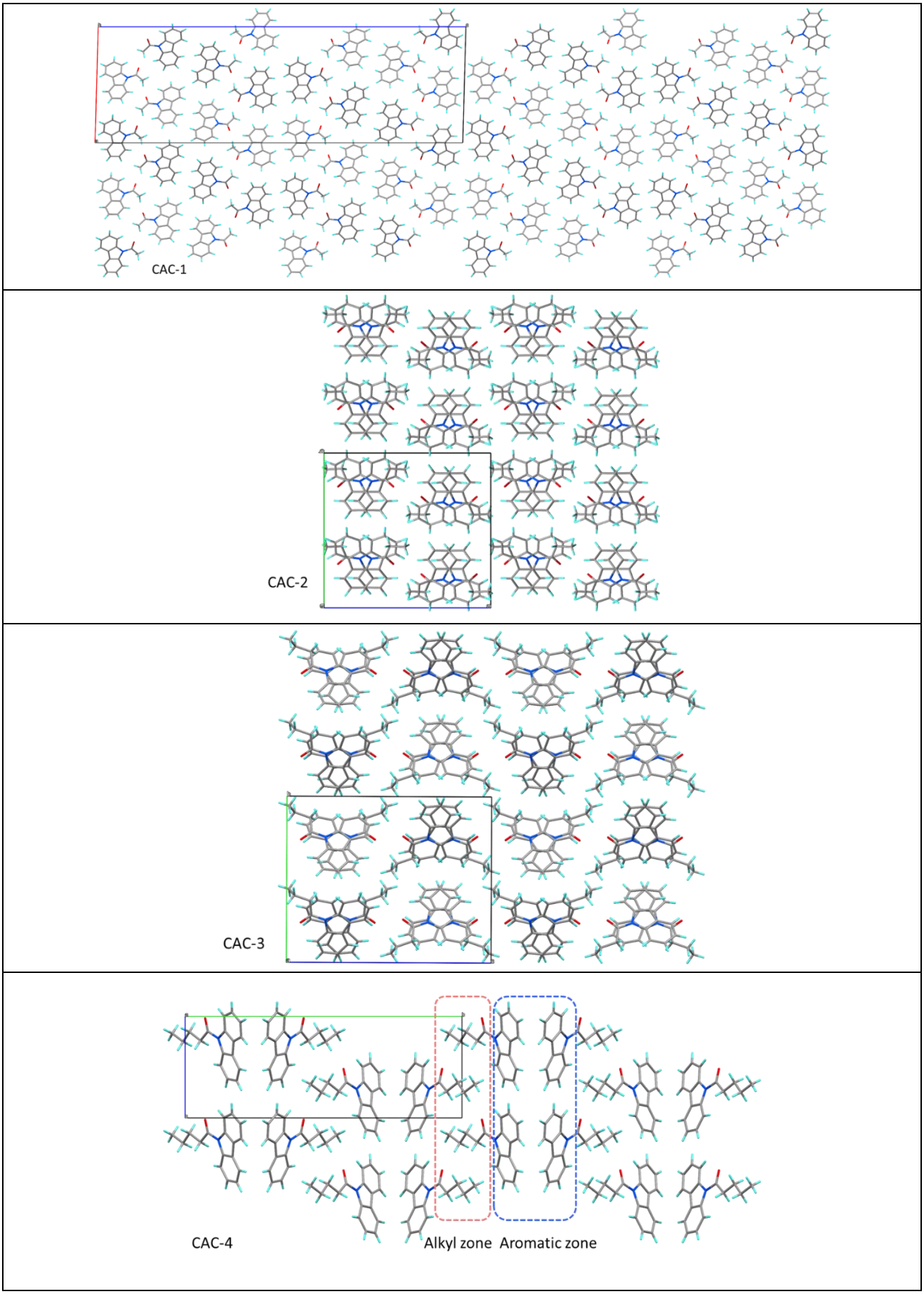

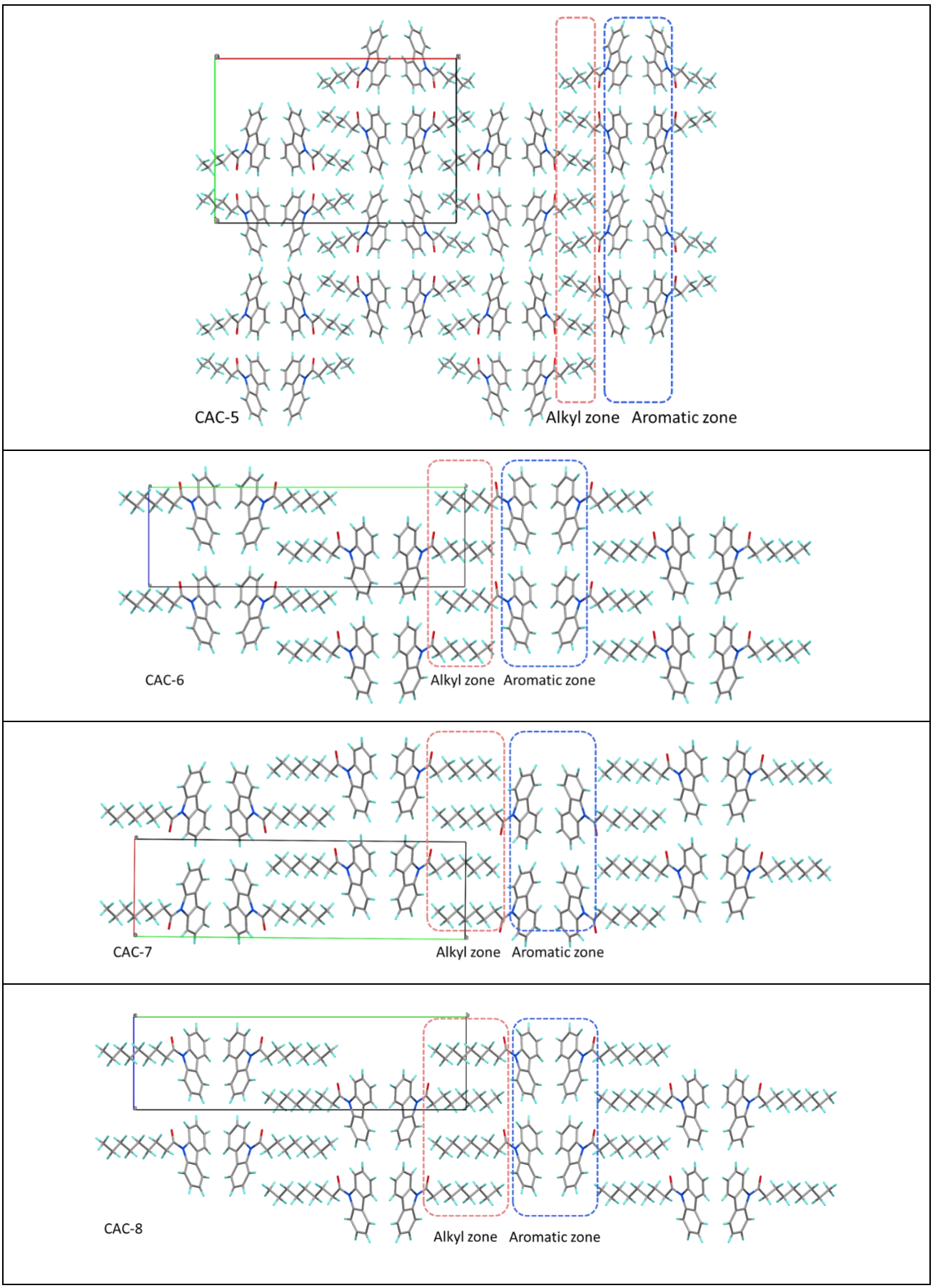
CAC-5
Alkyl zone
Aromatic zone
CAC-6
Alkyl zone
Aromatic zone
CAC-7
Alkyl zone
Aromatic zone
CAC-8
Alkyl zone
Aromatic zone

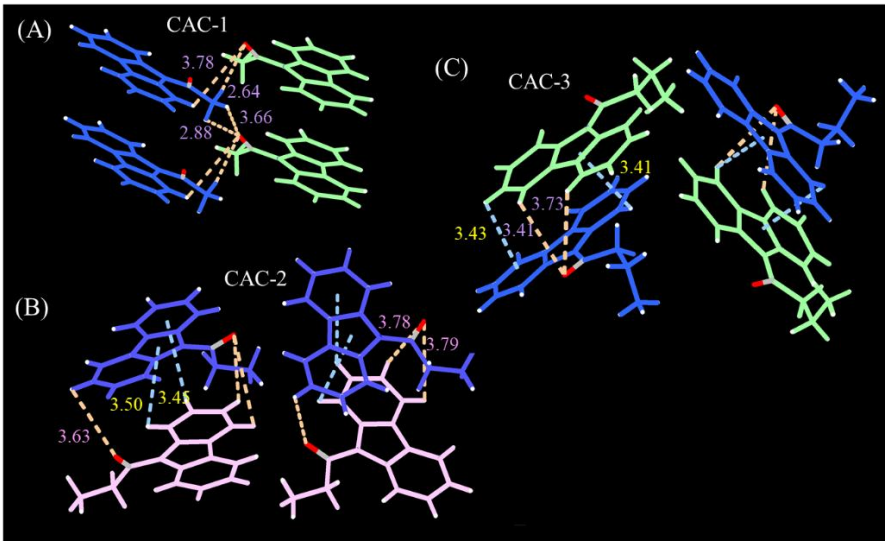

Fig. S42 Intermolecular interactions of CAC-*N* (*N* = 1 ~ 3).

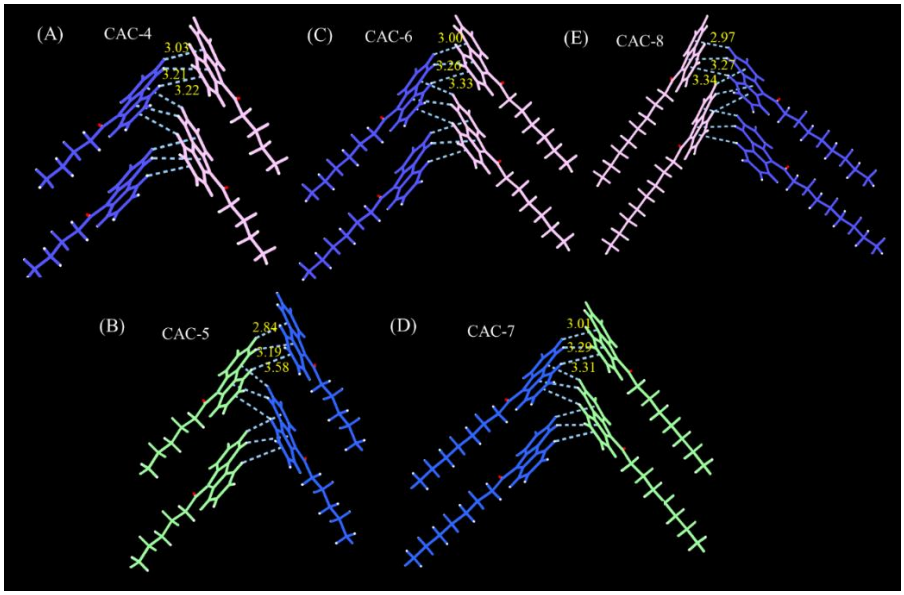

Fig. S43 Intermolecular interactions of CAC-*N* (*N* = 4 ~ 8).

Theoretical Calculation

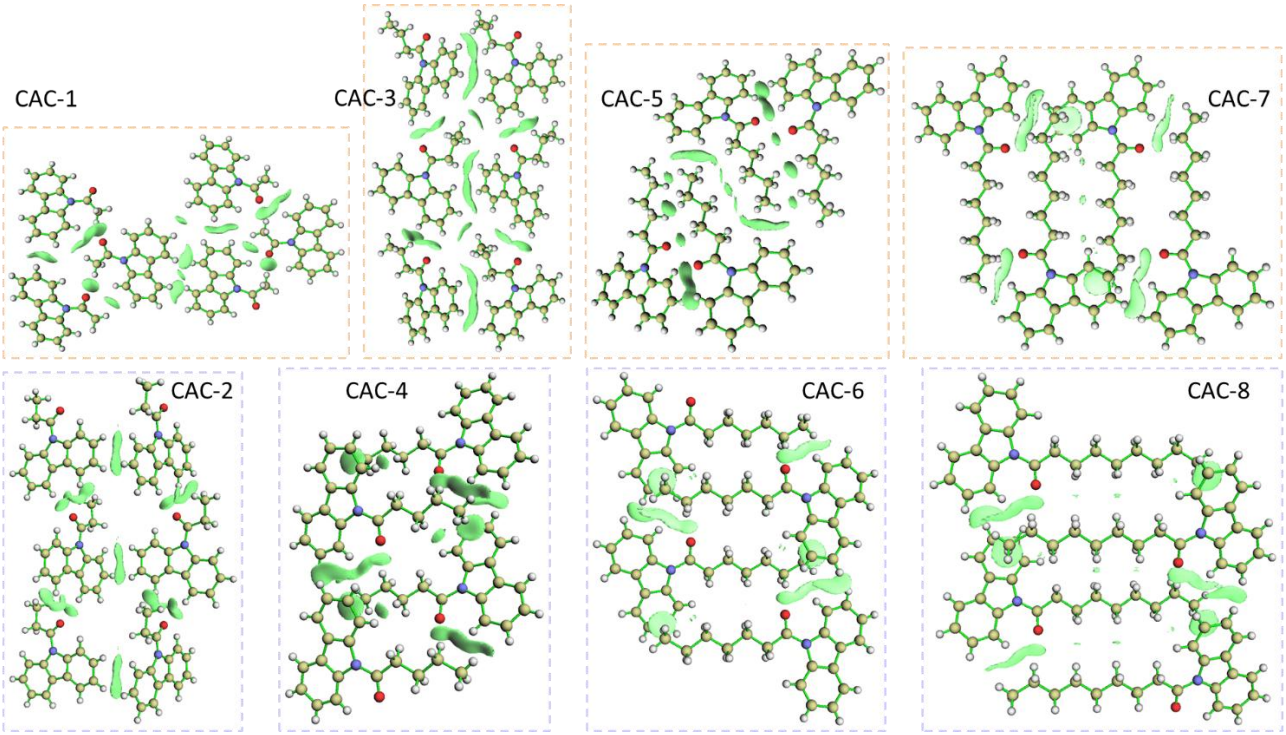

Fig. S44 Schematic visualization of intermolecular weak noncovalent interactions, which were calculated through independent gradient model (IGM) via Multiwfn 3.8 program.

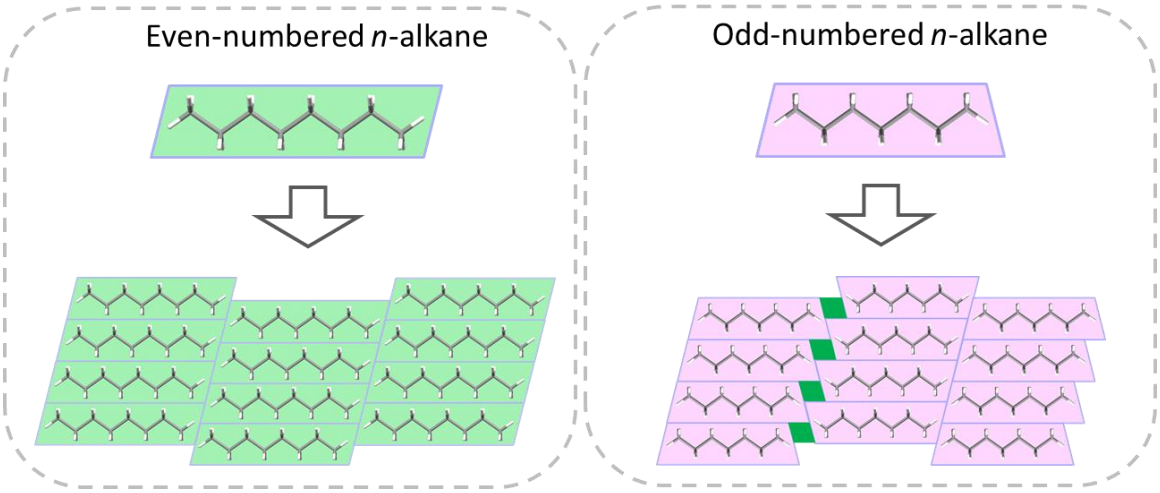

Fig. S45 Schematic representation of dense packing of even-numbered (left) and odd-numbered *n*-alkanes (right) in a two-dimensional projection.

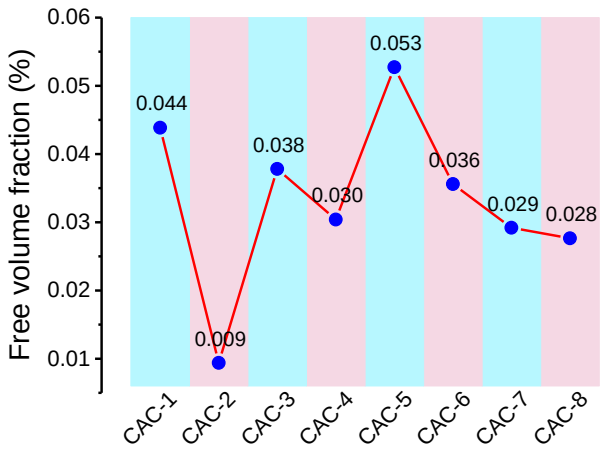

Fig. S46 Free volume fraction of eight crystals, calculated by Materials Studio program.

Table S5. Schematic presentation of free volume surface of eight crystals.

CAC-1	CAC-2
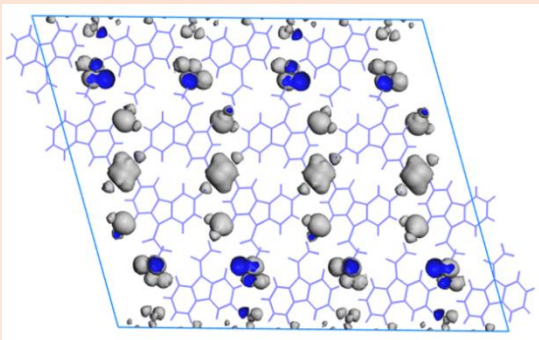	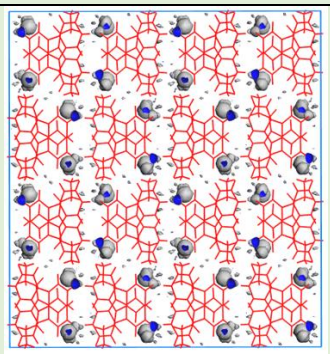
CAC-3	CAC-4
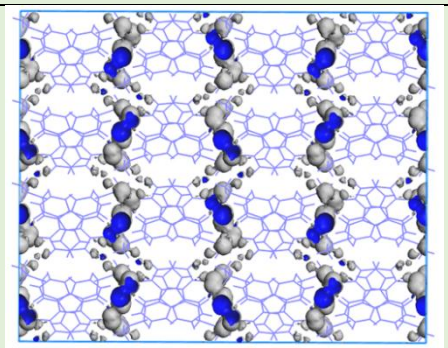	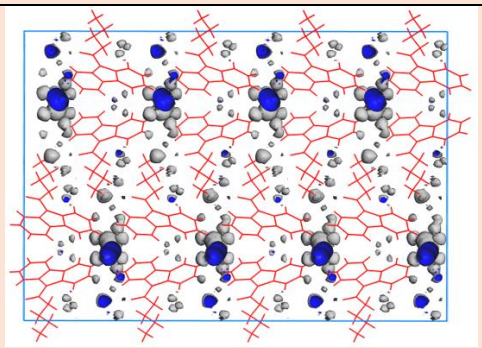
CAC-5	CAC-6
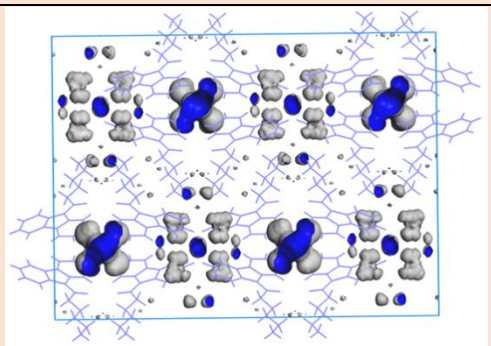	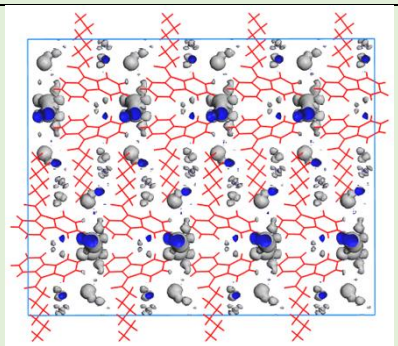
CAC-7	CAC-8

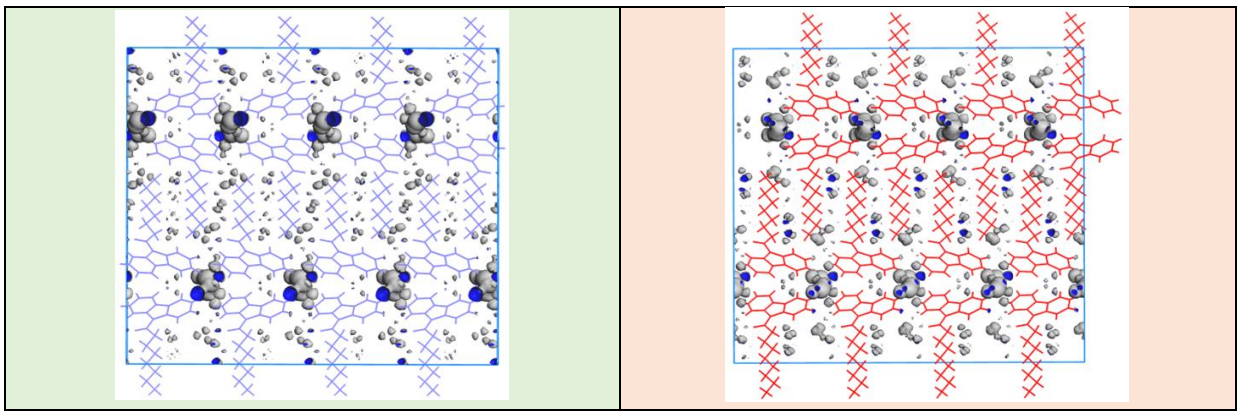

References

1. T. Lu, F. Chen, Multiwfn: A Multifunctional Wavefunction Analyzer. *J. Comput. Chem.* **2012**, *33*, 580-592.
2. Gaussian 09, Revision D.01, M. J. Frisch, G. W. Trucks, H. B. Schlegel, G. E. Scuseria, M. A. Robb, J. R. Cheeseman, G. Scalmani, V. Barone, B. Mennucci, G. A. Petersson, H. Nakatsuji, M. Caricato, X. Li, H. P. Hratchian, A. F. Izmaylov, J. Bloino, G. Zheng, J. L. Sonnenberg, M. Hada, M. Ehara, K. Toyota, R. Fukuda, J. Hasegawa, M. Ishida, T. Nakajima, Y. Honda, O. Kitao, H. Nakai, T. Vreven, J. A. Montgomery, Jr., J. E. Peralta, F. Ogliaro, M. Bearpark, J. J. Heyd, E. Brothers, K. N. Kudin, V. N. Staroverov, T. Keith, R. Kobayashi, J. Normand, K. Raghavachari, A. Rendell, J. C. Burant, S. S. Iyengar, J. Tomasi, M. Cossi, N. Rega, J. M. Millam, M. Klene, J. E. Knox, J. B. Cross, V. Bakken, C. Adamo, J. Jaramillo, R. Gomperts, R. E. Stratmann, O. Yazyev, A. J. Austin, R. Cammi, C. Pomelli, J. W. Ochterski, R. L. Martin, K. Morokuma, V. G. Zakrzewski, G. A. Voth, P. Salvador, J. J. Dannenberg, S. Dapprich, A. D. Daniels, O. Farkas, J. B. Foresman, J. V. Ortiz, J. Cioslowski, and D. J. Fox, Gaussian, Inc., Wallingford CT, 2013.